Universidade de Évora - Escola de Ciências e Tecnologia

Mestrado em Biologia da Conservação

Dissertação

Mapping the provision of seed-dispersal services mediated by birds in a quarry site to guide ecological restoration practices

Bruno Filipe Ferreira Ribeiro

Orientadores: |Pedro Alexandre Marques da Silva Salgueiro

Ana Sofia Xavier Pereira Diniz Sampaio

Évora 2023

Universidade de Évora - Escola de Ciências e Tecnologia

Mestrado em Biologia da Conservação

Dissertação

Mapping the provision of seed-dispersal services mediated by birds in a quarry site to guide ecological restoration practices

Bruno Filipe Ferreira Ribeiro

Orientadores: |Pedro Alexandre Marques da Silva Salgueiro

Ana Sofia Xavier Pereira Diniz Sampaio

Évora 2023

A dissertação foi objeto de apreciação e discussão pública pelo seguinte júri nomeado pelo Diretor da Escola de Ciências e Tecnologia:

Presidente	|	Paulo Sá-Sousa (Universidade de Évora)
Vogais	|	Pedro Alexandre Salgueiro (Universidade de Évora) (Orientador) Rui Lourenço (Universidade de Évora) (Arguente)

ABSTRACT

Restoring degraded sites to reverse some of the impacts of human resource extraction is paramount. Ecosystem services can be key to achieve self-sustainable systems through restoration, namely seed dispersal as it is provided by birds dispersing plants' seeds. As such, mapping these interactions between bird and plant species is essential to understand how and where to act to enhance this service in depleted areas. We constructed bipartite interaction networks and modelled network level metrics for the whole area, considering the effects of environmental factors to access seed dispersal service provision. We demonstrate that about 50% of the restored areas still present depleted seed dispersal service provision in comparison with other natural and semi-natural land uses, by presenting lower bird and plant diversity, and thus less linked and robust interaction networks. Furthermore, we were able to pinpoint these areas where restoration actions can now be deployed.

RESUMO: MAPEAMENTO DE SERVIÇOS DE DISPERSÃO DE SEMENTES MEDIADOS POR AVES NUMA ÁREA DE EXPLORAÇÃO DE INERTES PARA ORIENTAR MEDIDAS DE RESTAURO ECOLÓGICO

É fundamental restaurar locais degradados para reverter os impactos da extração de recursos. Os serviços ecossistémicos podem ser fundamentais para alcançar sistemas autossustentáveis através de restauro, nomeadamente a dispersão de sementes, sendo esta fornecida pelas aves que dispersam sementes das plantas. Assim, mapear estas interações entre espécies de aves e plantas é essencial para compreender como e onde agir para melhorar este serviço em áreas esgotadas. Construímos redes de interação bipartidas e modelamos métricas ao nível das redes para toda a área, considerando os efeitos dos fatores ambientais para avaliar a prestação deste serviço. Demonstramos que cerca de 50% das áreas restauradas ainda apresentam uma prestação deste serviço esgotada em comparação com outros usos naturais e seminaturais da terra, apresentando menor diversidade de aves e plantas e, consequentemente, redes de interação com menos conexões e menos robustas. Conseguimos também identificar as áreas onde as ações de restauro podem ser implementadas.

Index

1. Introduction

Restoration practices have been used to amend past disturbances on ecosystems and assist in their restoration. Traditional restoration efforts include revegetation with native and non-native plant species, to accelerate soil formation and reduce the impact of erosive agents, like rain and runoff (Werner et al., 2001). In the Mediterranean basin area, the introduction of Aleppo pine is common, aiming to assist seed establishment of native species, reduce soil erosion and to rapidly decrease the visual impact of the disturbed site (Pausas et al., 2004). However, the efficiency of these restoration practices needs to be ascertained, as these plantations may have a negative effect on plant and bird species diversity. Although soil fertility and water availability may increase at a relatively fast rate, in the long-term, increased runoff, sediment yield and water usage may hamper the development of the native shrub vegetation to a mature state. In most cases, the plantation areas never reach the same state as the natural mature shrublands, even after 40 years (Maestre and Cortina 2004). The plantation also affects the diversity of the faunal communities, due to the homogenization of the landscape, reducing habitat diversity, two key factors that negatively impact animal species (Lindenmayer and Hobbs, 2004).

Lately, much attention has been given to the role of ecosystems as providers of important services that affect human well-being and quality of life (Ayanu et al., 2012; M.E.A., 2005). These ecosystem services are maintained and are the result of the interactions between species in that ecosystem (Buckhard and Maes, 2017) and as such, they can be monitored as performance indicators for the effectiveness of the restoration practices and in decision-making (e.g., Dmitrakova et al., 2018; Salgueiro et al., 2020a; Ayanu et al., 2012). Consequently, evaluating if these restoration efforts comply with re-establishing these ecological processes is paramount, in order to accelerate the recovery of ecosystem functions in previously disturbed areas, as when these processes are restored, they will allow the whole system to regulate itself and discard the need of human intervention (Salgueiro et al., 2020b).

To obtain a more easily understandable picture of the state of the ecosystem services in an area, we rely on ecosystem service mapping to simplify the visualization of an otherwise hard to understand complex issue (Burkhard et al, 2012). Various methods are applied in order to extract the data used in this process, but the fastest and low-cost method that provides multitemporal data continuously in a large study area and surmounts the accessibility problem that field surveys may run into is remote sensing (Ayanu et al, 2012; Rozenstein et al, 2011; Nelson et al, 2009). By making use of remote sensing to map these services, we can establish more precise and effective decisions and policies (Malinga et

al., 2015) that can be applied in restoration practices by pinpointing where such services are depleted, providing the guidance on where and how to act to restore ecological function.

One of the ecosystem services that plays a key role in the restoration of damaged or destroyed habitats is animal mediated seed dispersal (zoochory), which allows various plants to colonize new, afar areas (Traveset et al., 2014). As many plant species often depend on these animals to extend their range and colonize new areas (Herrera, 2002; Salgueiro et al., 2020a), this is a crucial component of plant population dynamics (Levine and Murrell 2003), that contributes to increase ecosystem resilience (Nathan, 2006; Spiegel and Nathan, 2007; Rey and Alcántara, 2000).

Of the seed dispersing animals, birds are one of the most important groups (Whelan et al., 2008), often being considered good indicators of ecosystem service's provision (García et al., 2010). Birds are highly sensitive to disturbances in the ecosystems they are present as they embrace a wide range of ecological traits and niches, namely considering the way birds interact with plant species, their feeding behavior and phenology (spatio-temporal distribution) (Drapeau et al., 2000; Brotons et al., 2018). Many species of birds persist in human impacted habitats, although maybe only on a short term (Greenberg et al., 1997; Hughes et al., 2002), but can serve as vectors for restoration through seed dispersal (Sekercioglu, 2006).

In consequence of this tight link between birds and plants in seed dispersal, it is expected that changes in either community will affect the other and the network as a whole (Inger et al., 2015). As human activities highly threaten seed dispersal services, reducing the frequency of the bird-plant interactions (Neuschulz et al., 2016), studying these links is of an extreme importance to establish a map of the interaction network of a study area. The potential of seed-dispersing birds to assist revegetation of degraded areas by mining or quarrying activities is still neglected, since interactions between bird and plant communities in restored areas are poorly understood (Šálek, 2012; Makoto and Wilson, 2018).

As such, the goal of this study is to map seed dispersal services provisioned by birds in a restored quarry area and its vicinities, to guide more efficient and appropriate restoration and conservation practices regarding this ecosystem service. To attain this objective, we assessed the abundance and spatial distribution of fruit-bearing plants and bird seed-dispersers, and modeled interaction networks' metrics for the whole area, considering the effects of biotic and abiotic factors, including elevation, solar exposure, and vegetation greenery have on seed-dispersal service provision. We expect to pinpoint areas where seed-dispersion services provisioned by birds are depleted, identify restoration practices directed at ameliorating the provision of this service to further enable a self-sustainable and long-lasting restoration.

2. Methodology

2.1. Study area

This study was conducted at SECIL-Outão cement plant, located within the Arrábida Natural Park (classified in 1976), a calcareous mountainous area in the southwest of mainland Portugal (38◦29'24.51'' N, 8◦59'43.60''W), near the city of Setúbal. The area is characterized by a dry Mediterranean climate, a mid-latitude temperate climate which entails dry and hot summers and mildly cold wet winters according to the traditional climate classification (Köppen, 1900). This type of climate is prone to sclerophyllous vegetation, due to the water deficit suffered by the plants in the summer, which induces hydric stress. The landscape is typically characterized by the Mediterranean *maquis*, a dense semi-deciduous and evergreen sclerophyllous vegetation, like the kermes oak *Quercus coccifera;* the wild Mediterranean olive *Olea europaea* var. *silvestris*; the Mediterranean mastic tree *Pistacia lentiscus*; the strawberry tree *Arbutus unedo*; and the Juniper *Juniperus turbinata* (Catarino et al, 1982). The presence of non-native Aleppo pinewood *Pinus halepensis* is observed in this region, as well as mixed patches of oak-pine forest.

In the quarry, the exploitation of the limestone resources was conducted from top to bottom, forming various benches with 20 m (in older restored areas) or 10 m slope (in most recently restored areas) between them. In older restored areas, revegetation practices were conducted in benches since 1983 with soil landfilling (≈1-2 m depth) on the exposed rock and the plantation of native sclerophyllous vegetation and non-native Aleppo pine.

2.2. Experimental Design

We defined 32 points throughout the SECIL-Outão property (Figure 1), using satellite imagery and the QGIS software program (version 3.16.11 Hannover, QGIS Development Team, 2022). These points were no less than 200 meters apart and were distributed throughout the area with the support of a k-means clustering analysis of monthly Modified soil adjusted vegetation index (MSAVI2) and Normalized Difference Water Index (NDWI2) remote sensing images from the three previous years to cover different levels of vegetation structure. The points were also able to depict from a diversity of habitats, focusing on five types of land use: Mixed Forest, Quarry, Natural Shrubland, Pine Forest and Restored area. The Mixed Forest land use consisted of forest areas in valley composed of Portuguese oak (*Quercus faginea*) and Stone pine trees (*Pinus pinea*) and undercover dominated by dense and diverse fleshy fruit producing plant species. The quarry land use was related to the active limestone and marl resource extraction area. Pine forests referred to densely forested areas dominated by

Aleppo pines that cover much of the canopy. Restored areas corresponded to previously quarried areas that were meanwhile subjected to restoration practices.

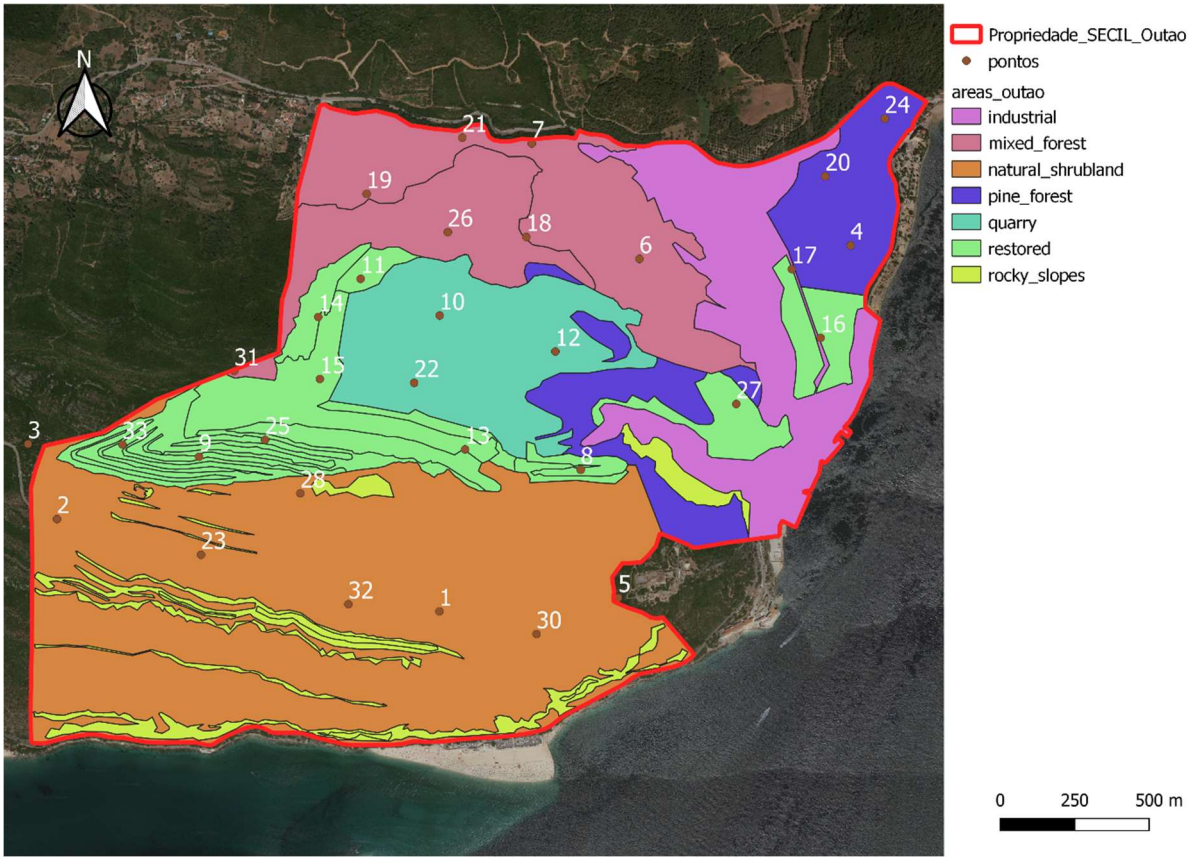

Figure 1: The 32 sampling points locations overlayed on top of a land use map of the SECIL-Outão property

2.3. Vegetation sampling

In each of the 32 sampling points, we surveyed sclerophyllous ripe fruit producing plant species present in each location using the linear interception method (Elzinga et al., 1998). Three 20 m transects were made at each sampling point, making a total of 60 meters sampled per point. In these transects, a straight line was drawn with the help of a measuring tape, and all individuals with a dimension greater than 30 cm (i.e., to exclude vegetation saplings) that crossed the vertical plane defined by the line were counted. For each plant, we determined if it was a fleshy fruit producing species and verified the presence of fruits on the plant. If present, the availability of fruits was counted as well as their state of maturation (ripe or unripe fruits). These samplings were conducted a total of five times, once every month, between September 2021 and January 2022.

2.4. Bird Sampling

Seed-disperser bird sampling was carried out at the same 32 sampling points defined for sampling vegetation. A 10-minute point count method (Bibby *et al.*, 2000) with a distance limit of 100 m was used to sample birds, always within the period of highest detectability (First 4 hours of sunlight) (Palmeirim and Rabaça, 1994) and with favorable weather conditions (Bibby *et al.*, 2000). These observations were conducted monthly between September 2021 and January 2022, with the same frequency and in the same days vegetation sampling occurred.

2.5. Interaction matrices

We computed virtual interaction matrices for each of the 32 sampling points based on real interaction data gathered by Sampaio et al. (2021) in the same study area. In Sampaio et al. (2021), bird fecal samples were collected by capturing birds using mist net traps, and its seed content was analyzed; bird abundances were registered following the same 10-minute point count protocol in a 50-meter radius and plant abundance (with ripe fruits) was registered by marking plants within the range of each bird point count. The vegetation species sampled were *Arbutus unedo*, *Daphne gnidium*, *Jasminum fruticans*, *Juniperus phoenicia*, *Lonicera implexa*, *Myrtus communis*, *Olea europea*, *Osyris alba*, *Rubus ulmifolius*, *Smilax aspera* and *Viburnum tinus*, with the bird species being *Turdus philomelos*, *Turdus merula*, *Curruca melanocephala*, *Sylvia atricapila*, *Erithacus rubecula*, *Cyanistes caeruleus*.

We first computed an interaction probability matrix compiling all information from interaction matrices of seed-dispersing birds and plants dispersed in Sampaio et al. (2021) study. The interaction probability matrix was computed by weighting the number of interactions of a bird species-plant species pair in relation to the total number of interactions of all pairs. Each value in the matrix thus represented the probability of a random dropping with seeds to express a given plant-bird interaction.

We also calculated the ratio of bird and ripe fruit plant species abundances between each of the 32 sampling points and the mean abundances registered in Sampaio et al. (2021). This procedure was replicated for each one of the five sampling months, using the formula below:

$$Pr = 1 + \frac{AR - AS}{AS}$$

Where Pr stands for the ratio between abundances, AR stands for abundance registered in this study and AS stands for abundance registered in the Sampaio et al. (2021) study.

For each of the sampled points at each month, we calculated the Probability Matrix Interaction (PMI) by multiplying the probability of interaction between the bird and plant species with ripe fruits established in Sampaio et al. (2021) by the abundances' ratios of bird and plant species with ripe fruits, with the formula we used is shown below:

$$PMI = IS \times PrB \times PrP$$

With PMI standing for Probability Matrix Interaction, IS stands for Interaction probability registered in the Sampaio et al. (2021) probability matrix, PrB standing for ratio between bird species abundances and PrP the ratio between plant species with ripe fruits' abundances.

The resulting matrices where then multiplied by the total number of interactions obtained in Sampaio et al. (2021) matrix (N=200), divided by the number of temporal replicates (in this case five months). This procedure was executed using the formula below:

$$EMI = \frac{N}{5} \times PMI$$

Where EMI stands for estimated matrix interaction, N stands for the total number of interactions registered in the Sampaio et al. (2021) study and PMI stands for probability matrix interaction.

This resulted in 160 estimated interaction matrices (5 monthly replicates in each of the 32 sampling points). Monthly results were then summed together per sampling point, leaving us with 32 estimated matrices. Estimating monthly instead of global interaction matrices avoided biases arising from extemporaneous interactions (i.e., considering a possible interaction when either a bird is absent, or a plant is not producing ripe fruits in a given month).

All species registered during fieldwork but not present in Sampaio et al. (2021), were excluded from the study. Nonetheless, our study captured 86% of bird species (6 species out of 7) and 88% in the case of plant species (14 out of 16 species) present in Sampaio et al. (2021).

2.6. Environmental variables

We used remote sensing variables (30-m resolution) related to the 32 observation points to model and predict the behavior of interaction network metrics, namely, the MSAVI2 and NDWI2. We also used other metrics pertaining to location and aspect, those being altimetry, ruggedness, slope, easting and northing.

MSAVI2 (Modified Soil-Adjusted Vegetation Index version 2) is a vegetation index being particularly good in areas where monitored vegetation alternates with a not-vegetated background (Qi et al.,

1994), and ranges between −1 and +1, moving towards higher values when biomass content of pixel increases (Montino et al., 2020).

NDWI2 (Normalized Difference Water Index 2) is an index used to obtain information on vegetation structure and its water content and ranges between -1 and +1 with higher values meaning better vegetation structure and more vegetation water content. These two indices permit the comparison of vegetation structure between different areas during our sampling period.

To obtain these indices we collected a set of Landsat 9 (L9) satellite multispectral images for each sampling month, and we averaged all values to retain a single image per index. NDWI was calculated in the following way:

$$\mathrm{NDWI} = \frac{\mathrm{NIR} - \mathrm{SWIR}}{NIR + SWIR}$$

where NIR stands for Near Infrared spectral band (band 5 of L9) and SWIR stands for Short-wave Infrared (band 6 of L9 images). As for MSAVI we used the formula bellow:

$$\mathrm{MSAVI2} = \frac{(2 * \mathrm{NIR} + 1) - \sqrt{(2 * NIR + 1)^{2} - (8 * (NIR - RED)}}{2}$$

Where NIR stands for Near Infrared spectral band (band 5 of L9 images) and RED concerns the red spectral band (band 3 of L9 images).

Easting and Northing are variables generated by the decomposition of the aspect of the area (which indicates the exposure of a slope in a degree format) applying the cosine and sine functions to build Northing and Easting, respectively.

Slope is also an important variable to deduce possible erosive runoff that can remove seeds and plantules from sites with more angular slopes (Thompson and Katul, 2009).

The aforementioned variables are summed in Table 1, with their respective description and range summarized.

Table 1: Chosen variables, their description and range

Variables	Description	Range
MSAVI2	vegetation biomass variation index in a landscape	−1 and +1, higher values meaning more biomass
NDWI2	vegetation water content	-1 and +1, higher values meaning more water content
Altimetry	altitude above sea level of the point in question	0 to 501m
Ruggedness	behavior of the variation of the altimetry in the points' surroundings (Robinson et al.,2019)	positive values meaning the point is higher than its surroundings
Slope	measures the angle of slope on which that point is located	0 to 40%
Easting	express the aspect (orientation) of the slope in degrees	-1 (west) to 1 (east)
Northing		-1 (south) to 1 (north)

These variables were adjusted using the "moving window" (mw) method, which smoothes the values of the sampled cell (in this case, the observation point). This is calculated with the r.neighbors function of GRASS extension in QGIS program (Geographical Resources Analysis Support System, Neteler et al., 2012). In this study, we selected a round moving window neighborhood of 49 cells (30 x 30 m each) for each observation point, translating to an area of 44100 square meters and a radius of 118 meters. This procedure allowed to conform the scale of the data variables to the data extracted on field, thus reducing the possible discrepancies between the precise location of the selected observation point and its surroundings.

2.7. Statistical Analysis:

2.7.1 Bipartite and network metrics

Firstly, a bipartite analysis of the virtual interaction matrices was employed as it provides a way to visualize interaction networks and calculate a series of metrics frequently used to describe its patterns. This approach makes it easier to visualize the data in a two-level network, in this case, plants whose seeds are dispersed (lower level) and birds who disperse those seeds (higher level), while the metrics summarize different aspects of the network's topology (Dormann et al., 2022).

We chose 14 metrics: web asymmetry, H2, Interaction Strength Asymmetry (ISA), Specialization Asymmetry (SA), weighted NODF (wNODF), modularity, linkage density, robustness HL (high-level) and robustness LL (low-level), and Shannon diversity. These comprise three specialization metrics (H2, ISA and SA), a nestedness metric (wNODF), a diversity metric (Shannon diversity), two metrics pertaining to the links in the network (linkage density and modularity), two robustness metrics (robustness higher level and robustness lower level) and web asymmetry.

In addition to the bipartite metrics, four metrics pertaining to species abundance were also obtained based on field data, using the methodology described in vegetation and bird sampling: mean bird abundance (m_aves), mean plant abundance (m_plants), bird abundance variation (sd_aves) and plant abundance variation (sd_plants).

The two mean abundance metrics were obtained by taking the maximum number of recorded individuals of each species in each month and adding them together, with the total being the sum of the maximum abundances in each month for that species. Subsequently, this sum was divided by 5, for the 5 months of observation and the number of observation points in each land use. The final result is a mean abundance of each species per land use. The formula we used is:

$$MA = \frac{\sum mma \times {}^{1}/_{5}}{N}$$

With MA being the mean abundance of each species per land use, mma being the monthly maximum abundance and N being the number of observation points in the specific land use.

The abundance variation metrics were obtained by calculating the standard deviation of the mean abundance metrics.

The response and purpose of each variable can be consulted in Table 2.

Table 2: Chosen metrics, their purpose and behavior, including value variation and its significance.

Metrics	Purpose	Response
Web asymmetry	Measures the disparity between the number of bird and plant species (Dormann et al., 2022)	positive values: more bird species; negative values: more plant species (Dormann et al., 2022)
H2	Calculates overall specialization of the network (Dormann et al., 2022)	higher values: less specialization; lower values: more specialization (Dormann et al., 2022)
ISA / SA	Explains how the specialization is distributed in the network (Dormann et al., 2022)	For ISA: higher values: more specialization occurs in bird species; lower values: more specialization occurs in plant species For SA: higher values: higher bird species specialization; lower values: lower bird species specialization (Dormann et al., 2022)
wNODF	Measures nestedness across the network (Dormann et al., 2022)	the higher the value, the higher the nestedness (Dormann et al., 2022), the lower the modularity and the higher the linkage density (Donatti et al.,2011)
Modularity	Measures how modular the network is	the higher the value, the more modules and less interaction links the network has
Linkage Density	Measures the density of interaction links between bird and plant species in the network	the higher the value, the less modules and more interaction links the network has
Robustness HL/LL	Measure the network's resistance to disturbances. The HL pertains to higher level (birds) and LL pretends to lower level (plants)	For HL: high linkage density/low modularity: higher robustness For LL: low linkage density/high modularity: lower robustness
Shannon diversity	Measures the diversity of species in the network	the higher the value, the higher the diversity, the higher number of species (Vollstädt et al., 2018), higher robustness
mean bird abundance/ mean plant abundance	Measure the sum of the maximum abundances of a species registered in an observation point divided by five samplings divided by the number of observation points of that land use	Birds: the higher the value, the higher the maximum number of birds Plants: the higher the value, the higher the maximum plants
bird abundance variation/ plant abundance variation	Measure the standard deviation of the maximum abundance of a species registered in an observation point divided by five samplings	Birds: the higher the value, the higher the standard deviation of maximum number of birds Plants: the higher the value, the higher the standard deviation of maximum number of plants having ripe fruits

Nestedness represents relationships between specialized and generalist species, with a core group of generalists all interacting with each other, with extreme specialists interacting only with generalist species (Bascompte et al. 2003). The increase in the nestedness value translates to a network with a higher composition of generalists, meaning that the variety and density of interactions in the network is higher. With more generalist species in a network, the more robust the network is to outside interference (extinction of one or more species for example), as the role of one depleted or eliminated species can more easily be assumed by others. If, in contrast, the network has a lower nestedness, the higher the degree of specialization of its species and the less resistant the network is to changes in its constituent species. (Atmar and Patterson, 1993; Burgos et al.,2007; Almeida-Neto et al., 2011).

This organization leads to highly asymmetrical interactions within the network and creates modules within which the community interacts around (Mariani et al.,2019). As such, modularity and

nestedness are tightly linked, as higher nestedness implies a convergence towards fewer modules (Donatti et al.,2011).

2.7.2. GLM and GAM modelling

After we chose which metrics to use, generalized linear and additive models (GLM and GAM) were conducted to assess the relation between the metrics and environmental variables. We conducted both types of models as some metrics displayed a non-linear response, something that the GLM is not fit to analyze, due to being specifically designed to model linear functions.

The modelling procedures themselves involved a two-step process. Firstly, each variable was tested for each metric by applying an univariated GAM using the *gam* function from the package 'mgvc' (Wood, 2023). The effective degrees of freedom (EDF) parameter was used to define the degree of linearity between the metric and environmental variables (e.g., if EDF = 1, a linear relationship existed, whereas if EDF > 2 the relationship was non-linear, and in subsequent models a smooth term was added to the variable). Very high EDF values could be problematic due to the very high non-linearity, so we defined a limit of 5 EDF as the maximum acceptable for this study. GCV scores, as an estimator of a prediction error, were also minimized in GAM models, since models with lower values are better fitted.

We used the Restricted Maximum Likelihood (REML) method for the modeling process, as it results in less biased estimates (Zuur et al; 2007) by separating the estimation of the fixed effects from the variance components (McNeish, 2017). We used gaussian error distributions for all dependent variables.

With the models' outputs obtained, the Akaike information criterion with a correction for small sample sizes (ΔAICc) was used to compare all candidate models. The models that passed the threshold of ΔAICc higher than 4 units when compared with the null models were discarded.

The best univariate models with a ΔAICc lower than 4 units were then tested in combinations. So, from the pool of approved models obtained in the prior steps, we tested every combination of models for every metric to determine which combination of variables had the best fit, based on the ΔAICc ranking.

The GAM tests were performed using the R-package mgcv (Mixed GAM Computation Vehicle). The R-package AICcmodavg was used to extract AICc values for all models.

2.7.3. Seed dispersal mapping

All models of each metric were extrapolated to the rest of the study area. With the predicted values from each metric's model spatially explicit throughout the entire area, we used the K-means algorithm to reduce the data from all metrics into coherent clusters. The K-means algorithm serves to cluster the extensive number of total results in a user determined number of classes, in accordance with the similarity between observations, as the observations cluster around fixed points that act as the center of the class (Likas et al., 2003). We determined a total number of four classes, as the separation between classes reached a point of quasi-stabilization at the 4-class point.

By mapping the k-means results, we obtained a detailed map of the study area with the clusters colored by the k-means defined class, as well as the behavior of each observation class in accordance with each metric (called ridge plots), thus making possible the evaluation of the response of each metric to each cluster.

Superimposing the land use boundaries, were able to determine the proportion of each class in every land use via a bar graph, thus making possible the comparison between land uses in respect to area-wide metrics data.

All statistical analyses were conducted using the program R v.4.2.0 using RStudio 2022.02.03 Build 492 (R Development Core Team 2022).

3. Results

3.1 General results

The land uses presented a distinct composition of plant and bird species and their abundances. The best performing land use in terms of bird species abundance was the natural shrubland, followed by mixed forest, pine forest, restored and quarry, being the least abundant.

For plants species, the land use with the most abundance of plants having ripe fruits was the mixed forest, followed by pine forest, natural shrubland and the restored area. We found no fleshy fruited plant species on observations conducted in the quarry land use.

These results can be consulted in figures 2 and 3.

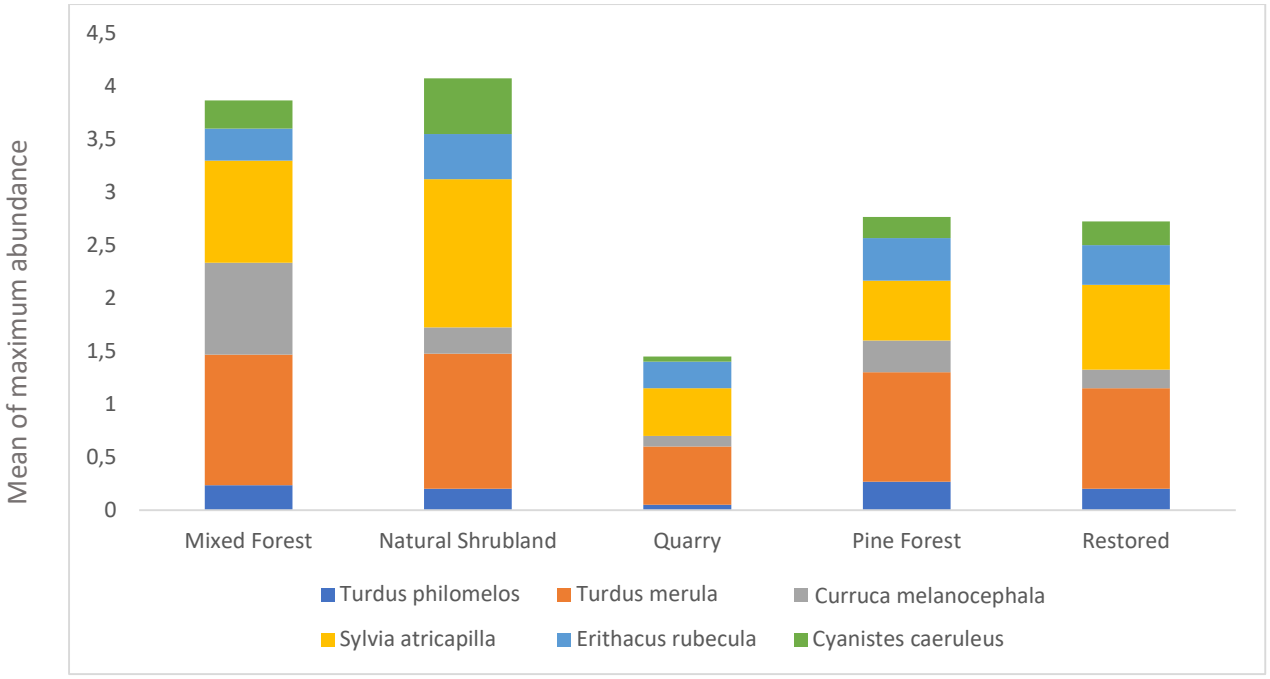

Figure 2: Distribution of the mean of the maximum abundances by species per land use per month, weighted in accordance with the number of observation points in each land use.

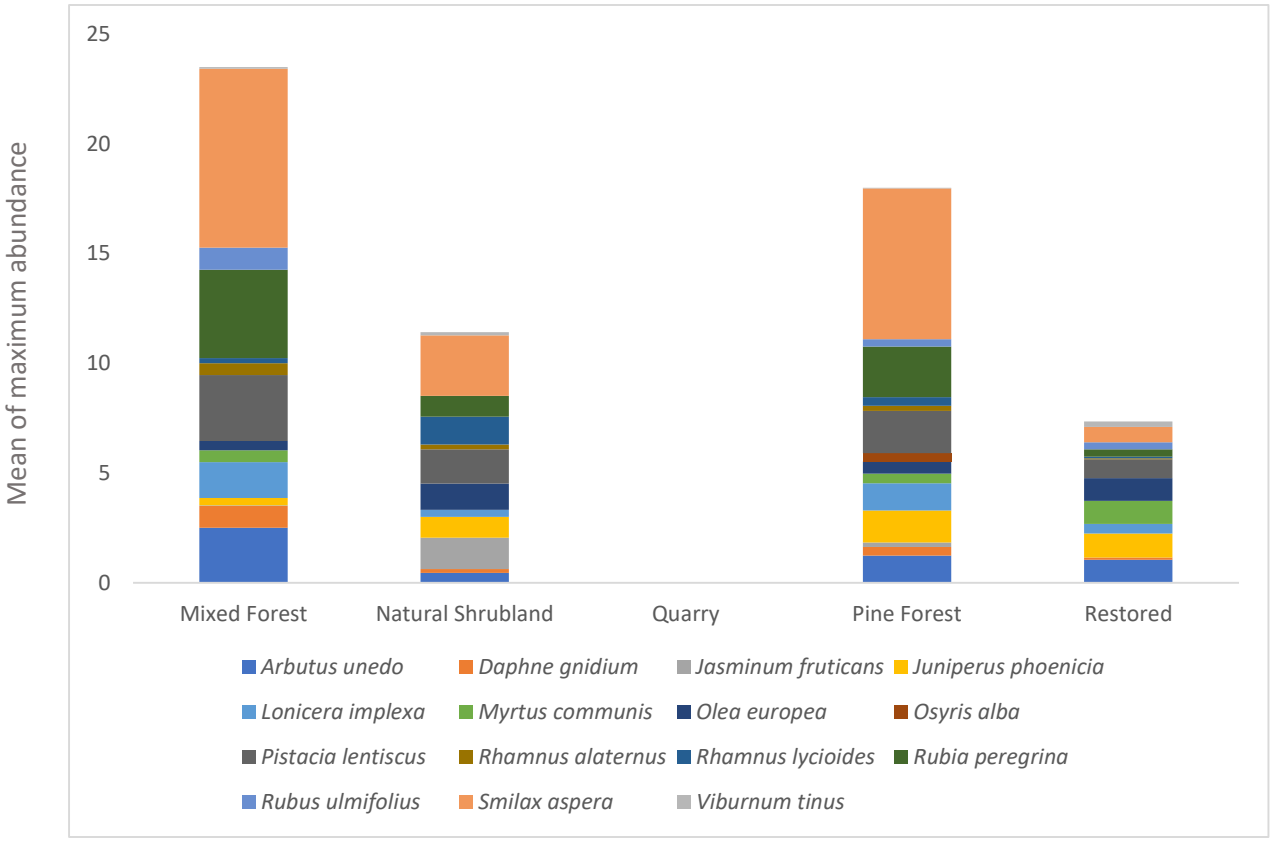

Figure 3: Distribution of the mean of the maximum abundances of ripe fleshy fruit producing plant species per land use per month, weighted in accordance with the number of observation points in each land use.

3.2 Modelling

The best models for each metric were determined and can be consulted in Table 3. Most of these models use the variable NDWI2 alone or paired with altimetry, with or without the smoothing factor. Only the metrics interaction strength asymmetry, specialization asymmetry, mean bird abundance and bird abundance variation displayed models with variables better adjusted other than NDWI2, being MSAVI2, ruggedness, MSAVI2 and MSAVI2+easting, respectively. The models chosen and their parameters can be consulted in table 3 below.

Table 3: Chosen final models and their respective parameter's values. The s() factor indicates that the model has a smoothness factor applied

Metric	Model Chosen	Explained Deviance	F value	p-value
web asymmetry (weba)	NDWI2	0.369	-3.821	0.001
weighted NODF (wNODF)	s(NDWI2)	0.438	9.803	0.000
interaction strength asymmetry (ISA)	MSAVI	0.440	-2.660	0.014
specialization asymmetry (SA)	rugged	0.252	-2.840	0.009
linkage density (linkd)	NDWI2	0.584	32.840	0.000
Shannon diversity (Shdiv)	NDWI2+ Altim	0.512	1.978	0.059
			-3.341	0.003
H2	NDWI2	0.166	-2.278	0.031
nº Species LL (nspLL)	NDWI2	0.427	3.337	0.001
robustness HL (robHL)	s(altim)+ NDWI2	0.466	4.009	0.019
			2.396	0.025
robustness LL (robLL)	s(altim)+ s(NDWI2)	0.743	8.428	0.000
			3.392	0.043
modularity (modul)	NDWI2	0.137	-2.033	0.052
mean plant abundance (m_plant)	NDWI2	0.751	9.508	0.000
plant abundance variation (sd_plant)	NDWI2+ s(altim)	0.567	2.971	0.006
			3.878	0.022
mean bird abundance (m_aves)	MSAVI	0.792	10.702	0.000
bird abundance variation (sd_aves)	MSAVI+ easting	0.620	5.862	0.000
			3.579	0.001

As presented in table 3, most of the models chosen (n=10) have explained deviance values ranging between 25% and 62%, indicating that for the majority of metrics the respective models are reasonably or even well-adjusted to the data. Exceptions to that are the models of H2 and modularity metrics, with explained deviances below 15%. On the other hand, mean bird abundance, mean plant abundance and robustness LL explained deviances were above 70%, meaning these metrics' models are very well adjusted to the data.

The F and p-values pertain to the specific variables in the model. These parameters indicate the validity of the statistical analysis, and the ones presented show that the metrics have marginal or even sound statistical validity, with most metrics presenting a p-value lower than 0.05, which means it is statistically significant, with the two exceptions (the models pertaining to modularity and Shannon diversity) being only marginally above 0.05.

Among the metrics that appear most in the models with high significance are NDWI2, MSAVI2 and altimetry.

3.3 Clustering

The map showing the total number of observations colored by clustering class, the ridge plots table as well as the bar graph illustrating the percentage of each class in each land use were obtained and enable a more intuitive look at the clustering classes and land uses.

In Figure 4, the layout of the clustering classes throughout the study area can be observed. Here, we can clearly see the location of the active quarry, as well as the factory and other industrial zones, making up the majority of the class 1 (purple) areas, and the clustering of class 4 (yellow) in the mixed forest land use, as well as a great class 2 (blue) extension speckled with some class 3 (green) to the south of the quarry, corresponding to the natural shrubland land use. We can also observe, although less detailed, the patch of class 2 and 3 on the northwest of the study area corresponding to the majority of the pine forest land use.

Interestingly, we can see a strip of class 2 and class 1 separating the quarry and the mixed forests land uses corresponding to some of the restored land use, evidencing the stark difference between this land use and the mixed forest.

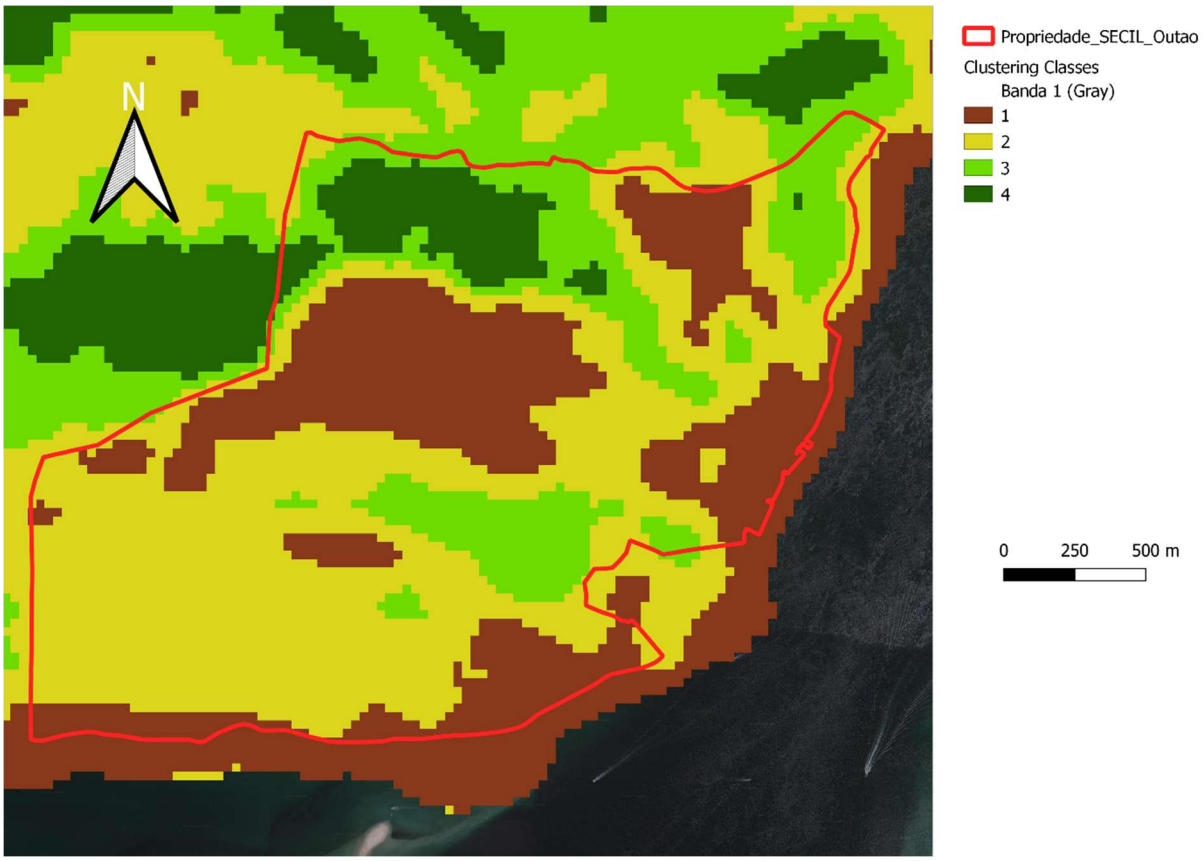

Figure 4: Map of the study area displaying the distribution of observations per cluster class: purple is class 1; blue is class 2; green is class 3 and yellow is class 4.

The ridge plots showed some marked differences across metrics. The number of bird and plant individuals tend to be lower in class 1 clusters and higher in class 4 clusters, while clusters 2 and 3 show intermediate values. This sets a tendency, as metrics such as linkage density, robustness and Shannon diversity display the same pattern. These positive trends are inversed in metrics like modularity, interaction strength asymmetry, web asymmetry, H2 and specialization asymmetry all tending to have lower values in class 4 cluster than class 1.

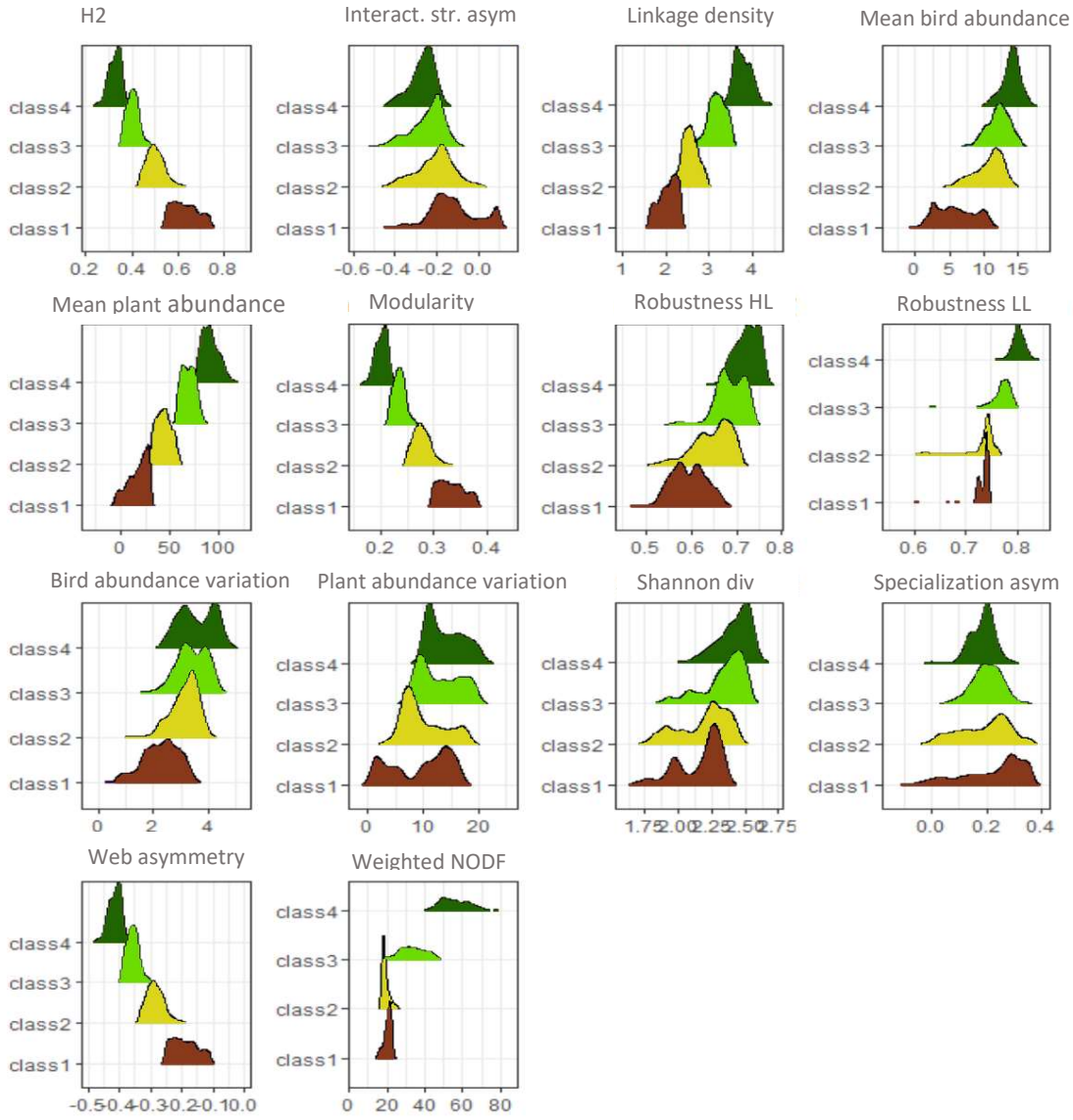

Figure 5: Ridge plot graph table, displaying each metric's tendency and behavior per clustering class.

In terms of clusters associations with land use, class 4 clusters were only registered in the Mixed Forest land use, which also shows lower percentages of class 2 and almost no class 1 cluster. In reverse, the Quarry land use presents almost no other class than class 1, with only around 6% represented class 2 observations (Figure 6).

Most interestingly for this study in particular is the composition of the restored land use's composition, with an almost complete 50% split between class 1 and 2, with a residual presence of class 3 observations.

The two other land uses (Natural shrubland and Pine Forest) present a composition between the restored and mixed forest land uses, with the percentage of class 3 growing considerably and the diminishing of class 1 percentage. This transition is more accentuated in the Pine Forest land use, with comparable percentages of class 2 and 3 and about 10% of class 1 composition, and less evident in the Natural Shrubland land use, as class 2 observations constitute the uncontested majority of the percentage registered, with similar percentages (about 15% each) of class 1 and class 3 observations.

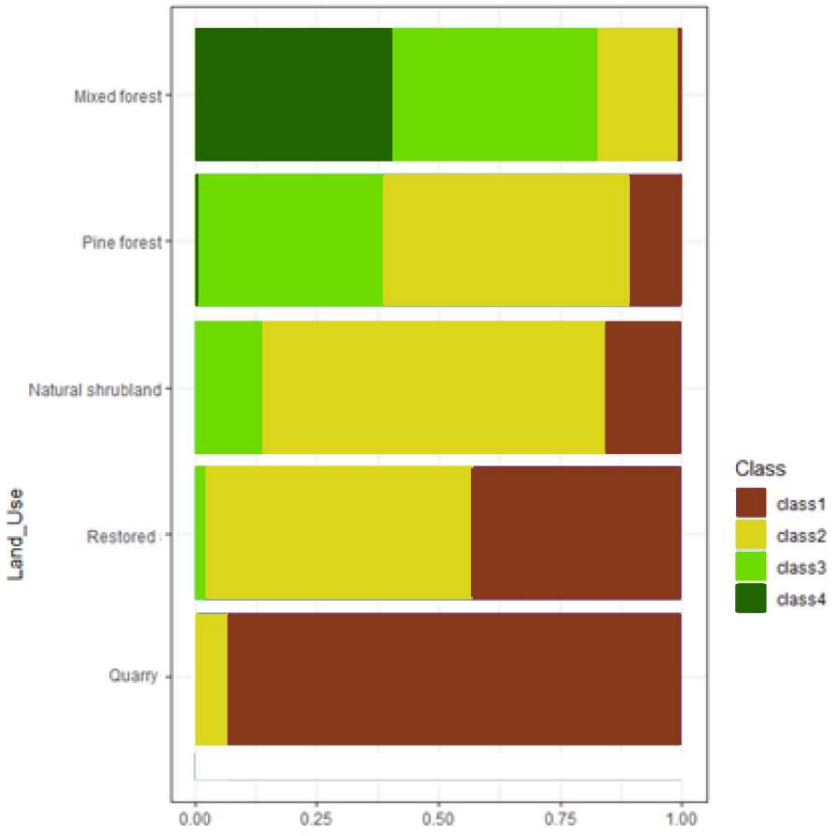

Figure 6: Bar graph displaying each land use's composition in terms of clustering class.

4. Discussion

4.1 Metrics

We can establish that the interaction networks analyzed in the observations of class 4 were the most robust, diverse and present greater number of links, followed by classes 3 and 2, with class 1 presenting the highest modularity, highest asymmetries and less diversity and robustness of the four. The metrics illustrated a ranking of clustering classes, from 1 to 4, in terms of the quality of the networks and ecosystems observed in the areas associated with the respective classes. Our seed dispersal service map revealed that the Restored land use is mainly composed of classes 1 and 2, with a negligeable percentage of class 3, with this low performance only being beaten by the Quarry land use, which represents the active mining sites. In stark contrast, the Mixed Forest land use was composed primarily of classes 3 and 4, with about 10% class 2, and even less class 1. Using this information, we can conclude that the land use with better interaction networks was Mixed Forest, followed by Pine Forest, Natural Shrubland and finally the Restored and Quarry land uses.

The clustering classes composition of the Restored land use describes a type of ecosystem with its services depleted in almost 50% of the area, as indicated primarily by the high modularity, asymmetry and specialization and low diversity and links of its interaction networks and supported by the field metrics abundance of bird and plant individuals as well. All these metrics evidence a smaller and sparser vegetation structure, with less resources for birds, thus lower bird abundance, ultimately resulting in less robust interaction networks present in these areas. On the contrary, the composition of the Mixed Forest land use revealed a healthier set of metric trends, being the opposite of those seen in the Restored land use, with ecosystem services showing superior results in terms of diversity, abundance and linkage density, meaning more robust interaction networks. (Garcia et al., 2018; Heleno et al., 2013; Traveset et al., 2015; Sebastián-González, 2017; Timóteo et al., 2018).

The Quarry land use presented no surprises in its results, as no fleshy fruit producing plant species were observed in it.

The Pine Forest land use presented the second-best clustering class distribution. There is still roughly 10% of class 1 composition, but class 3 comprises more than 30% of the land use's composition. This land use is characterized by high pine cover, and it was expected to perform worse than the more autochthonous mixed forest, as the pine trees compete for sunlight, water, nutrients and space with the smaller native plants, while developing faster than the native plants (Maestre and Cortina 2004).

The Natural Shrubland land use was mostly represented by class 2 observations, with roughly equal percentage of class 1 and class 3. Notably, there were no class 4 observations on this land use's

composition. This land use presents a lower vertical complexity, lower humidity and water content, as the land use's potential does not benefit the establishment of a bird and vegetation community like the one present in the valleys of Mixed Forests or even those found in the Pine Forests, (Fabijańczyk et al., 2022; Borgogno-Mondino et al., 2020) as it is located in significantly more rocky, higher and steep areas.

Although the Restored land use presents significantly more percentage of class 1 observations than the Natural Shrubland and only a negligible percentage of class 3, the Natural Shrubland continues to be the realistic goal of restoration, as the Restored land use's edaphoclimatic characteristics are closest to those found in the Natural Shrubland, even bosting similar rocky and steep cliffs, it is apparent that the goal of restoration must be to approximate the Restored land use's composition and interaction network's performance to those of the Natural Shrubland

4.2 Models

The chosen metrics were valid to this study, as demonstrated by the models being quite adjusted to the data we collected, as most models explained 35% or higher of the deviance.

Secondly, as the metrics display some correlation while describing network structure, the models tested generally depended on the same parameters, with NDWI, MSAVI and altimetry being the most represented. As a mountainous site, altimetry had a huge impact on water availability, soil conditions and solar exposure, and consequently, the types of vegetation change according to the specific zone it was located, leading to different humidity and vegetation cover levels, as different types of habitats exist at different altitudes (Huang et al., 2020). This was, of course, complemented with the other parameters, like slope and its orientation (northing and easting) and ruggedness of the terrain (Huang et al., 2020). That is why, in some metrics modeled using NDWI, MSAVI and altimetry, non-linear relations needed to consider to accurately model its behavior.

The fact that most metrics had their models based on these three parameters was very interesting and express the general tendency that all the metrics followed. In areas with higher levels of humidity (measured by MSAVI), high levels of more developed vegetation (measured by NDWI) can develop, meaning more plant abundance and more plant species diversity (Fabijańczyk et al., 2022; Borgogno-Mondino et al., 2020), which provided more possible interactions, attracting bird species, increasing the linkage density, the diversity and decreasing the modularity and web asymmetry of that network. With more vegetation cover, more humidity is retained. These areas are typically located in valleys,

where humidity is higher and where the soil is more productive and deep, boosting the viability of more plants (Fabijańczyk et al., 2022; Borgogno-Mondino et al., 2020).

As shown, NDWI, MSAVI and altimetry parameters are intrinsically connected and the metrics which have their chosen models based on them are, as well, tightly linked and express the same or directly inverse tendency (like linkage density and modularity). Regarding this, we can confidently access the satisfactory adjustment of the chosen models to the metrics and the data obtained.

Although most metrics are exclusively modeled by NDWI, MSAVI or altimetry, or some combination of these three, two metrics are modeled by different parameters: Specialization asymmetry and bird standard deviation models were best fitted by ruggedness and easting, respectively. Specialization asymmetry's relation with ruggedness can be linked to the fact that the depleted ecosystem services are located primarily in the quarry and restored land uses, precisely where the landscape is more rugged and where, in the case of the quarry land uses, there were not any fleshy fruit producing plants observed. The bird standard deviation's metric relation with easting can be attributed to the location of the most east facing zones of the study area, which include a good portion of the highest rated land use, mixed forest and also some of the pine forest land use.

These chosen models are not without some limitations. Firstly, although quite well adjusted to the data collected, the explained deviance and behavior supplied by these models could be higher if some other unknown parameters were chosen. Alas, we chose the parameters that seemed to make sense in the context of the study area.

Secondly, some observed species were not considered in this study, as parity between this study's species and those observed in Sampaio et al. (2021) was imperative, as the interaction matrices we constructed were based on the interactions observed in that study. As such, some potential interactions were not considered here due to the lack of interaction data on those specific species from previous studies.

4.3 Future Implications

The results obtained in this study evidence that the provision of seed-dispersal ecosystem services in the restored area is below what was expected when compared to natural and semi-natural areas. Although the clustering classes distribution in the restored land use is quite similar to the natural shrubland, the former has a very sizable minority percentage of class 1 cluster, with almost no class 3 and no class 4 at all.

With this paradigm, it seems the most logical procedure is to approximate the restored area composition to the one found in the natural shrubland areas. To achieve this, we need to transform around 20% of the class 1 composition to class 2 and increase the percentage of the almost non-existent class 3 to about 12%.

We can conclude that the restored land use has a higher web asymmetry and higher modularity. This reveals an imbalance in the network due to less plant species richness and abundance present than those necessary to establish a linkage density of a robust interaction network. As such, restoration measures need to be directed at promoting a plant composition similar to the one found in the natural shrubland.

The problems that hinder the establishment of this plant composition can be attributed to an assortment of factors, some even pertaining to the establishment of Aleppo pine (*Pinus halepensis*) in former restoration practices back in the 1980's and 1990's in the steps of the restored areas. This practice was common in revegetation projects at that time in the Iberian Peninsula to reduce soil erosion (Pausas et al., 2004), enhance seedling establishment of the native species and to rapidly reduce the visual impact of the exposed rock slopes in the landscape (Werner et al., 2001). This practice, however, may also have had the unfortunate consequence of hindering the growth of understory native plants and bushes, since in the low soil quality zones the native vegetation may have problems in competing with the Aleppo pine, resulting in a scant understory cover (Bellot et al., 2004; Nunes et al., 2014). Thus, a lower abundance of plants and lower diversity of plant species, resulted in a lower variety of resources and number of seeds to attract bird species.

As discussed in the analysis of the models, vegetation cover, humidity and altimetry are the three most important factors influencing the condition of the interaction networks. The restoration practices can focus on increasing water availability and water retention to enable a better vegetation cover. With this, the gradual extraction pines seems to be necessary, as to let the native plants take its place. With the native plants increasing in number and diversity, the bird species present will also increase and boost the natural restoration of the areas, and, hopefully, culminate in a status similar to the one found in the natural shrubland areas.

Acknowledgements

We acknowledge SECIL-Outão for funding this study and granting access to the study area.

I would like to thank Francesco for the Landsat 9 (L9) data he provided for this study, as well as Pedro and Ana for the unwavering support and invaluable help in the data collecting, analysis and in the writing of this dissertation, as well as André for help in the field work and the tips for writing.

I would also like to thank my friends that never stopped encouraging me and asking for the progress on writing this dissertation, in particularly Inês for the tips and the mutual support we shared by writing a dissertation, Cristiana and Sara for pulling my ears and constantly saying "you can do it", my two best friends, Bernardo and Daniel, for worrying and caring for my mental disposition and once again, encouraging me, my family, in particular my mother, father and sister, for their support and constant encouragement, as well as my girlfriend Beatriz, for showing pride in every step of my journey of writing a dissertation.

References

Almeida-Neto, M., & Ulrich, W. (2011). A straightforward computational approach for measuring nestedness using quantitative matrices. Environmental Modelling & Software, 26(2), 173-178. Toruń, Poland.

Atmar, W. & Patterson, B. (1993). The measure of order and disorder in the distribution of species in fragmented habitat. Oecologia, 96: 373–382. Chicago, USA.

Ayanu, Y. Z., Conrad, C., Nauss, T., Wegmann, M. & Koellner, T. (2012). Quantifying and mapping ecosystem services supplies and demands: a review of remote sensing applications. Environmental science & technology, 46(16), 8529-8541. Bayreuth, Germany.

Bascompte, J., Jordano, P., Melian, C.J. & Olesen, J.M. (2003) The nested assembly of plant-animal mutualistic networks. Proceedings of the National Academy of Sciences of the United States of America, 100, 9383 –9387. USA.

Bellot, J., Maestre, F.T., Chirino, E., Hernandez, N. & de Urbina, J.O. (2004). Afforestation with *Pinus halepensis* reduces native shrub performance in a Mediterranean semiarid area. Acta Oecologica 25 (1–2), 7–15. Alicante, Spain

Bibby, C.J., Burgess, N.D., Hill, D.A. & Mustoe, S. (2000). Bird Census Techniques. Academic Press, London, UK. 302 pp.

Borgogno-Mondino, E., de Palma, L., & Novello, V. (2020). Investigating Sentinel 2 Multispectral Imagery Efficiency in Describing Spectral Response of Vineyards Covered with Plastic Sheets. Agronomy, 10(12), 1909. Italy.

Brotons, L., Herrando, S., Sirami, C., Kati, V., & Díaz, M. (2018). Mediterranean forest bird communities and the role of landscape heterogeneity in space and time. *In*: Mikusinski, G., Roberge, J.M., Fuller, R.J. (Eds.), Ecology and Conservation of Forest Birds. Cambridge University Press, Cambridge, UK, pp. 318–349.

Burgos, E., Ceva, H., Perazzo, R. P., Devoto, M., Medan, D., Zimmermann, M., & Delbue, A. M. (2007). Why nestedness in mutualistic networks? Journal of Theoretical Biology, 249(2), 307-313. Buenos Aires, Argentina.

Burkhard, B., Kroll, F., Nedkov, S., & Müller, F. (2012). Mapping ecosystem service supply, demand and budgets. Ecological Indicators, 21, 17-29. Kiel, Germany

Burkhard & B., Maes, J. (2017) (Eds.) Mapping Ecosystem Services. Pensoft Publishers, Sofia, 374 pp. Hannover, Germany

Catarino, F.M., Correia, O.A. & Correia, A.I.V. (1982). Structure and dynamics of Serra da Arrábida mediterranean vegetation. Ecol. Mediterr. 8 (1), 203–222. Saint-Maximin, France

Dmitrakova, Y., Rodina, O., Alekseev, I., Polyakov, V., Petrova, A., Pershina Ivanova, E. A., Abakumov, E.V. & Kostecki, J. (2018). Restoration of soil-vegetation cover and soil microbial community at the Pechurki limestone quarry (Leningrad region, Russia). Soil Science Annual 69 (4), 272–286.

Donatti, C. I., Guimarães, P. R., Galetti, M., Pizo, M. A., Marquitti, F. M. & Dirzo, R. (2011). Analysis of a hyper-diverse seed dispersal network: modularity and underlying mechanisms. Ecology Letters, 14(8), 773-781. Brazil.

Dormann, C. F., Fruend, J., Gruber, B., Dormann, M. C. F. & LazyData, T. R. U. E. (2014). Package 'bipartite'. Visualizing bipartite networks and calculating some (ecological) indices (Version 2.17). (R Foundation for Statistical Computing). Freiburg, Germany.

Drapeau, P., Leduc, A., Giroux, J., Savard, J., Bergeron, Y. & Vickery, W. (2000). Landscape-scale disturbances and changes in bird communities of boreal mixed-wood forests. Ecological Monographs 70 (3), 423–444. Montreal, Canada.

Elzinga, C.L., Salzer, D.W. & Willoughby, J.W. (1998). Measuring and Monitoring Plant Populations. Technical Reports 1730-1. Bureau of Land Management, Denver, Colorado, USA, USDI, BLM, pp. 101–173, 172.

Fabijańczyk, P. & Zawadzki, J. (2022). Spatial correlations of NDVI and MSAVI2 indices of green and forested areas of urban agglomeration, case study Warsaw, Poland. Remote Sensing Applications: Society and Environment, 26, 100721. Warsaw, Poland.

Gann, G., McDonald, T., Walder, B., Aronson, J., Nelson, C., Jonson, J., Hallet, J.G., Eisenberg, C., Guariguata, M.R., Liu, J., Hua, F., Echeverría, C., Gonzales, E., Shaw, N., Decleer, K. & Dixon, K.W. (2019). International principles and standards for the practice of ecological restoration. Restoration Ecology 27. Australia.

García, D., Donoso, I., & Rodríguez-Pérez, J. (2018). Frugivore biodiversity and complementarity in interaction networks enhance landscape-scale seed dispersal function. Functional Ecology, 32(12), 2742-2752. Oviedo, Spain.

García, D., Zamora, R. & Amico, G.C., (2010). Birds as suppliers of seed dispersal in temperate ecosystems: conservation guidelines from real-world landscapes. Conservation Biology 24 (4), 1070–1079. Oviedo, Spain.

Greenberg, R., Bichier, P., & Sterling, J. (1997). Bird populations in rustic and planted shade coffee plantations of eastern Chiapas, Mexico. Biotropica, 29(4), 501-514. Washington DC, USA.

Heleno, R. H., Ramos, J. A., & Memmott, J. (2013). Integration of exotic seeds into an Azorean seed dispersal network. Biological Invasions, 15, 1143-1154. Coimbra, Portugal.

Herrera, C.M. (2002). Seed dispersal by vertebrates. In: Herrera, C.M., Pellmyr, O.M. (Eds.), Plant–animal Interactions: An Evolutionary Approach. Blackwell Publishing, Oxford, pp. 185–208. Seville, Spain.

Huang, C., Yang, Q., Guo, Y., Zhang, Y., & Guo, L. (2020). The pattern, change and driven factors of vegetation cover in the Qin Mountains region. Scientific Reports, 10(1), 20591. China.

Hughes, J. B., Daily, G. C., & Ehrlich, P. R. (2002). Conservation of tropical forest birds in countryside habitats. Ecology Letters, 5(1), 121-129. Stanford, California, USA.

Hurvich, C. M., & Tsai, C. L. (1989). Regression and time series model selection in small samples. Biometrika, 76(2), 297-307. USA.

Inger, R., Gregory, R., Duffy, J.P., Stott, I., Vorisek, P. & Gaston, K.J. (2015). Common European birds are declining rapidly while less abundant species' numbers are rising. Ecology Letters 18, 28–36. United Kingdom.

Levine, J. M., & Murrell, D. J. (2003). The Community-Level Consequences of Seed Dispersal Patterns. Annual Review of Ecology, Evolution, and Systematics, 34, 549–574. Santa Barbara, California, USA.

Likas, A., Vlassis, N., & Verbeek, J. J. (2003). The global k-means clustering algorithm. Pattern recognition, 36(2), 451-461. Ioannina, Greece.

Lindenmayer, D. B., & Hobbs, R. J. (2004). Fauna conservation in Australian plantation forests–a review. Biological Conservation, 119(2), 151-168. Australia.

Maestre, F. T., & Cortina, J. (2004). Are Pinus halepensis plantations useful as a restoration tool in semiarid Mediterranean areas? Forest ecology and management, 198(1-3), 303-317. Alicante, Spain.

Makoto, K. & Wilson, S.D. (2018). When and where does dispersal limitation matter in primary succession? Journal of Ecology 107 (2), 559–565. Japan.

Mariani, M. S., Ren, Z. M., Bascompte, J., & Tessone, C. J. (2019). Nestedness in complex networks: observation, emergence, and implications. Physics Reports, 813, 1-90. China.

McNeish, D. (2017). Small sample methods for multilevel modeling: A colloquial elucidation of REML and the Kenward-Roger correction. Multivariate behavioral research, 52(5), 661-670. North Carolina, USA.

Mello, M. A. R., Marquitti, F. M. D., Guimarães, P. R., Kalko, E. K. V., Jordano, P., & de Aguiar, M. A. M. (2011). The modularity of seed dispersal: differences in structure and robustness between bat–and bird–fruit networks. Oecologia, 167(1), 131-140. Ulm, Germany.

Millennium ecosystem assessment, M. E. A. (2005). Ecosystems and human well-being (Vol. 5, pp. 563-563). Washington, DC: Island press.

Nathan, R., (2006). Long distance dispersal of plants. Science 313, 786–788. Israel.

Nelson, E., Mendoza, G., Regetz, J., Polasky, S., Tallis, H., Cameron, D., ... & Shaw, M. (2009). Modeling multiple ecosystem services, biodiversity conservation, commodity production, and tradeoffs at landscape scales. Frontiers in Ecology and the Environment, 7(1), 4-11. United Kingdom.

Neteler, M., Bowman, M. H., Landa, M., & Metz, M. (2012). GRASS GIS: A multi-purpose open-source GIS. Environmental Modelling & Software, 31, 124-130. Italy.

Neuschulz, E.L., Mueller, T., Schleuning, M. & Böhning-Gaese, K. (2016). Pollination and seed dispersal are the most threatened processes of plant regeneration. Science Repository 6 (1), 1–6. Frankfurt am Main, 60325, Germany

Nunes, A., Oliveira, G., Cabral, M. S., Branquinho, C., & Correia, O. (2014). Beneficial effect of pine thinning in mixed plantations through changes in the understory functional composition. Ecological engineering, *70*, 387-396. Lisbon, Portugal.

Palmeirim, J.M. & Rabaça, J.E. (1994) A method to analyze and compensate for time-of-day effects on bird counts. Journal of Field Ornithology 65(1): 17-26. Portugal.

Pausas, J.G., Bladé, C., Valdecantos, A., Seva, J.P., Fuentes, D., Alloza, J.A. & Vallejo, R., (2004). Pines and oaks in the restoration of Mediterranean landscapes of Spain: new perspectives for an old practice—a review. Plant Ecology 171 (1), 209–220. Valencia, Spain.

Principal Component Analysis in R Tutorial, by Luke Hayden, available at https://www.datacamp.com/tutorial/pca-analysis-r#introduction-to-pca ,accessed on 21/09/2022.

QGIS Geographic Information System. Open-Source Geospatial Foundation Project.

Rey, P.J. & Alcántara, J. (2014). Effects of habitat alteration on the effectiveness of plant-avian seed dispersal mutualisms: consequences for plant regeneration. Perspectives in Plant Ecology, Evolution and Systematics 16 (1), 21–31. Jaén, Spain.

Robinson, T. P., Di Virgilio, G., Temple-Smith, D., Hesford, J., & Wardell-Johnson, G. W. (2018). Characterization of range restriction amongst the rare flora of Banded Ironstone Formation ranges in semiarid south-western Australia. Australian Journal of Botany, 67(3), 234-247. Australia.

Rozenstein, O., & Karnieli, A. (2011). Comparison of methods for land-use classification incorporating remote sensing and GIS inputs. Applied Geography, 31(2), 533-544. Negev, Israel.

Šálek, M., (2012). Spontaneous succession on opencast mining sites: implications for bird biodiversity. Journal of Applied Ecology 49 (6), 1417–1425. Prague, Czechia.

Salgueiro, P.A., Prach, K., Branquinho, C. & Mira, A., (2020a). Enhancing biodiversity and ecosystem services in quarry restoration – challenges, strategies, and practice. Restoration Ecology 28, 655–660. Évora, Portugal.

Salgueiro, V., Silva, C., Eufrázio, S., Salgueiro, P.A., Vaz, P.G., (2020b). Endozoochory of a dry-fruited tree aids quarry passive restoration and seed soaking further increases seedling emergence. Restoration Ecology 28, 668–678. Évora, Portugal.

Sampaio, A. D., Pereira, P. F., Nunes, A., Clemente, A., Salgueiro, V., Silva, C., ... & Salgueiro, P. A. (2021). Bottom-up cascading effects of quarry revegetation deplete bird-mediated seed dispersal services. Journal of Environmental Management, *298*, 113472. Évora, Portugal.

Sebastián-González, E. (2017). Drivers of species' role in avian seed-dispersal mutualistic networks. Journal of Animal Ecology, 86(4), 878-887. São Paulo, Brazil.

Sekercioglu, C. H. (2006). Increasing awareness of avian ecological function. Trends in ecology & evolution, 21(8), 464-471. Stanford, California, USA.

Spiegel, O. & Nathan, R. (2007). Incorporating dispersal distance into the disperser effectiveness framework: frugivorous birds provide complementary dispersal to plants in a patchy environment. Ecology Letters 10 (8), 718–728. Jerusalem, Israel.

Thompson, S., & Katul, G. (2009). Secondary seed dispersal and its role in landscape organization. Geophysical Research Letters, 36(2). Western Australia, Australia.

Timóteo, S., Correia, M., Rodríguez-Echeverría, S., Freitas, H., & Heleno, R. (2018). Multilayer networks reveal the spatial structure of seed-dispersal interactions across the Great Rift landscapes. Nature Communications, 9(1), 140. Coimbra, Portugal.

Traveset, A., Heleno, R., & Nogales, M. (2014). The ecology of seed dispersal. In Seeds: the ecology of regeneration in plant communities (pp. 62-93). Wallingford UK: CABI.

Traveset, A., Olesen, J. M., Nogales, M., Vargas, P., Jaramillo, P., Antolín, E. & Heleno, R. (2015). Bird–flower visitation networks in the Galápagos unveil a widespread interaction release. Nature communications, 6(1), 6376. Mallorca, Spain.

Vollstädt, M. G., Ferger, S. W., Hemp, A., Howell, K. M., Böhning-Gaese, K., & Schleuning, M. (2018). Seed-dispersal networks respond differently to resource effects in open and forest habitats. Oikos, 127(6), 847-854. Frankfurt am Main, Germany

Werner, C., Clemente, A., Correia, P., Lino, P., Máguas, C., Correia, A. & Correia, O. (2001). Restoration of disturbed areas in the mediterranean — a case study in a limestone quarry. In: Breckle, S.W., Veste, M., Wucherer, W. (Eds.), Sustainable Land Use in Deserts. Springer, Berlin, Heidelberg, Germany.

Whelan, C., Wenny, D. & Marquis, R. (2008). Ecosystem services provided by birds. Annals of the New York Academy of Sciences 1134 (1), 25–60. Illinois, USA.

Wood, S. (2023). Mixed GAM Computation Vehicle with Automatic Smoothness Estimation. Edinburgh, United Kingdom.

Zuur, A. F., Ieno, E. N., & Smith, G. M. (2007). Analysing ecological data (Vol. 680). New York: Springer. Darmstadt, Germany.

Annexes

Tables I trough XVI: Univariated Model selection tables for each metric, showing the AICc values used in the selecting process. Green lines mean the model has a lower AICc value than the null model, red lines mean a higher AICc value than the null model and yellow lines represent the null models.

Web asymmetry

Variable	AICc	Rsq	Expl,Dev	GCV	edf	P	ΔAIC
mw_NDWI2	-31,836	0,236695	0,264966	-15,8357	NA	0,005067	0
s(mw_NDWI2)	-31,8358	0,236696	0,264968	-13,7354	1,000052	0,005069	0,00018
mw_slope	-29,4028	0,167397	0,198234	-10,7353	NA	0,017585	2,43318
mw_MSAVI2b	-28,8421	0,150556	0,182017	-14,7963	NA	0,02357	2,99387
mw_rugged	-28,7021	0,146297	0,177915	-10,0016	NA	0,025372	3,13393
s(mw_slope)	-28,4907	0,20454	0,253975	-12,7461	1,677956	0,037017	3,34533
s(mw_rugged)	-27,9701	0,206079	0,26137	-12,6006	1,880343	0,046048	3,86591
s(mw_MSAVI2b)	-27,9404	0,308653	0,392957	-12,7489	3,29243	0,033462	3,89558
s(mw_altim)	-26,941	0,204199	0,270755	-12,1627	2,258097	0,062736	4,89499
Null	-25,7366	0	0	-12,4116	NA	NA	6,09946
mw_altim	-25,2324	0,033675	0,069465	-6,07273	NA	0,175368	6,60359
Easting	-25,0805	0,028418	0,064402	-11,0426	NA	0,192546	6,75552
s(easting)	-25,0804	0,028418	0,064403	-10,5989	1,000025	0,192554	6,75561
Northing	-23,2866	-0,03587	0,002499	-10,2545	NA	0,800571	8,54941
s(northing)	-21,8238	0,195975	0,313726	-9,53606	3,954209	0,219852	10,0122

Weighted NODF

Variable	AICc	Rsq	Expl,Dev	GCV	edf	P	ΔAIC
s(mw_NDWI2)	239,9208	0,37359	4,38E-01	111,5684	2,779201	0,007226	0
mw_NDWI2	242,369	0,174094	2,05E-01	111,4737	NA	0,015638	2,4482
mw_altim	245,0934	0,089694	1,23E-01	119,4357	NA	0,066794	5,1726
s(mw_altim)	245,0938	0,089693	1,23E-01	114,839	1,000095	0,066811	5,173
mw_MSAVI2b	245,7949	0,066597	1,01E-01	112,7138	NA	0,099049	5,8741
s(mw_MSAVI2b)	245,7963	0,066602	1,01E-01	115,1647	1,000355	0,099128	5,8755
Null	246,2614	0	0,00E+00	118,7302	NA	NA	6,3406
Northing	247,6518	0,002599	3,95E-02	115,5383	NA	0,310391	7,731
s(northing)	248,5245	0,031045	8,44E-02	115,9496	1,487675	0,415988	8,6037
mw_rugged	248,696	-0,0353	3,05E-03	118,7904	NA	0,780326	8,7752
s(mw_rugged)	248,6994	-0,03527	3,12E-03	116,5116	1,001031	0,781897	8,7786
Easting	248,7692	-0,03801	4,36E-04	116,1019	NA	0,916014	8,8484
mw_slope	248,772	-0,03811	3,36E-04	118,4172	NA	0,926191	8,8512
s(mw_slope)	248,7727	-0,03811	3,44E-04	116,5469	1,000182	0,927009	8,8519
s(easting)	249,0186	0,045682	1,12E-01	116,0981	1,866947	0,408874	9,0978

Interaction strength asymmetry

Variable	AICc	Rsq	Expl,Dev	GCV	edf	P	ΔAIC
mw_MSAVI2b	-15,1224	0,195943	2,26E-01	-8,42638	NA	0,010622	0
s(mw_MSAVI2b)	-15,1221	0,195945	2,26E-01	-5,97551	1,000088	0,010626	0,000276
mw_rugged	-15,0749	0,194577	2,24E-01	-3,67467	NA	0,010884	0,047522
s(mw_rugged)	-15,0748	0,194576	2,24E-01	-5,95344	1,000012	0,010885	0,047582
mw_slope	-14,8388	0,187757	2,18E-01	-3,97347	NA	0,012287	0,283616
s(mw_slope)	-14,8388	0,187757	2,18E-01	-5,84383	1,000007	0,012288	0,283651
mw_NDWI2	-12,1378	0,105502	1,39E-01	-6,69016	NA	0,051036	2,98457
s(mw_NDWI2)	-10,8878	0,263063	3,52E-01	-4,85992	3,271169	0,067116	4,234606
s(mw_altim)	-10,6909	0,194741	2,69E-01	-4,63363	2,50098	0,100233	4,431558
null	-10,4793	0	1,16E-16	-5,05546	NA	NA	4,643095
northing	-9,21577	0,007108	4,39E-02	-3,72161	NA	0,284688	5,906643
s(northing)	-8,87107	0,193052	2,87E-01	-3,69581	3,134186	0,159107	6,251344
easting	-8,79561	-0,0079	2,94E-02	-3,48171	NA	0,382764	6,326805
s(easting)	-8,75733	-0,00741	3,04E-02	-3,0381	1,012492	0,389597	6,365077
mw_altim	-8,55382	-0,01665	2,10E-02	1,670904	NA	0,461794	6,568594

Specialization asymmetry

Variable	AICc	Rsq	Expl,Dev	GCV	edf	P	ΔAIC
s(mw_altim)	-19,7613	5,03E-01	5,72E-01	-8,83453	3,753694	0,001316	0
mw_rugged	-16,4586	2,52E-01	2,80E-01	-4,31709	NA	0,003784	3,302683
s(mw_rugged)	-16,4585	2,52E-01	2,80E-01	-6,59587	1,000013	0,003785	3,30274
mw_slope	-16,0193	2,41E-01	2,69E-01	-4,52155	NA	0,004719	3,741981
s(mw_slope)	-16,0192	2,41E-01	2,69E-01	-6,39191	1,000016	0,00472	3,742053
mw_MSAVI2b	-11,0022	9,15E-02	1,25E-01	-6,51344	NA	0,064776	8,75902
s(mw_MSAVI2b)	-11,0022	9,15E-02	1,25E-01	-4,06257	1,000014	0,064779	8,759074
northing	-10,4858	7,46E-02	1,09E-01	-4,31126	NA	0,086408	9,275484
s(northing)	-10,4855	7,46E-02	1,09E-01	-3,82278	1,00007	0,086423	9,275715
mw_altim	-10,0669	6,06E-02	9,54E-02	0,968422	NA	0,109715	9,694402
null	-9,77872	-2,22E-16	-1,13E-16	-4,71767	NA	NA	9,982538
mw_NDWI2	-7,77076	-1,96E-02	1,81E-02	-4,66259	NA	0,494634	11,99049
s(mw_NDWI2)	-7,77073	-1,96E-02	1,81E-02	-2,56224	1,000007	0,494639	11,99052
easting	-7,43771	-3,18E-02	6,37E-03	-2,85126	NA	0,686367	12,32354
s(easting)	-6,64058	-8,38E-03	4,43E-02	-2,4617	1,409881	0,709228	13,12067

Linkage density

Variable	AICc	Rsq	Expl,Dev	GCV	edf	P	ΔAIC
mw_NDWI2	40,56193	0,568155	5,84E-01	17,77759	NA	2,20E-06	0
s(mw_NDWI2)	41,3712	0,601699	6,31E-01	19,51093	1,965354	1,27E-05	0,80927
mw_MSAVI2b	56,34659	0,24115	2,69E-01	24,75565	NA	4,67E-03	15,78466
s(mw_MSAVI2b)	56,3468	0,24115	2,69E-01	27,20653	1,000057	4,67E-03	15,78487
mw_altim	59,03528	0,164668	1,96E-01	33,05155	NA	1,84E-02	18,47335
s(mw_altim)	59,03617	0,164677	1,96E-01	28,45484	1,000287	1,85E-02	18,47424
null	62,60994	0	0,00E+00	30,184	NA	NA	22,04801
northing	63,77934	0,010441	4,71E-02	30,16897	NA	2,67E-01	23,21741
s(northing)	63,77954	0,01044	4,71E-02	30,65746	1,000044	2,67E-01	23,21761
mw_slope	64,31512	-0,00868	2,87E-02	32,77656	NA	3,89E-01	23,75319
s(mw_slope)	64,31522	-0,00868	2,87E-02	30,90621	1,00002	3,89E-01	23,75329
mw_rugged	64,64914	-0,02078	1,70E-02	33,34006	NA	5,08E-01	24,08721
s(mw_rugged)	64,64938	-0,02078	1,70E-02	31,0613	1,000056	5,08E-01	24,08745
easting	65,11092	-0,03776	6,79E-04	30,83203	NA	8,95E-01	24,54899
s(easting)	65,62002	-0,02831	1,74E-02	31,26499	1,199076	9,07E-01	25,05809

Shannon diversity

Variable	AICc	Rsq	Expl,Dev	GCV	edf	P	ΔAIC
mw_NDWI2	22,7797	0,27844	3,05E-01	9,521554	NA	0,002302	0
s(mw_NDWI2)	22,77977	0,27844	3,05E-01	11,6219	1,000015	0,002303	7E-05
mw_altim	26,64675	0,171577	2,02E-01	18,01402	NA	0,016344	3,86705
s(mw_altim)	26,64682	0,171576	2,02E-01	13,41732	1,000016	0,016345	3,86712
mw_MSAVI2b	29,58645	0,079871	1,14E-01	12,33131	NA	0,078957	6,80675
null	30,45394	0	0,00E+00	14,68021	NA	NA	7,67424
northing	31,04475	0,030679	6,66E-02	14,97077	NA	0,18494	8,26505
s(northing)	31,0449	0,030679	6,66E-02	15,45925	1,000034	0,184952	8,2652
s(mw_MSAVI2b)	31,06885	0,124327	1,85E-01	14,72875	1,874614	0,177755	8,28915
easting	31,65083	0,009468	4,62E-02	15,29699	NA	0,272266	8,87113
s(easting)	31,65095	0,009469	4,62E-02	15,74064	1,000032	0,27228	8,87125
mw_rugged	32,87858	-0,03493	3,40E-03	18,58944	NA	0,768202	10,09888
s(mw_rugged)	32,8791	-0,03493	3,41E-03	16,31067	1,000157	0,768427	10,0994
mw_slope	32,95281	-0,03768	7,54E-04	18,21549	NA	0,889666	10,17311
s(mw_slope)	32,95292	-0,03768	7,56E-04	16,34513	1,00003	0,889755	10,17322

H2

Variable	AICc	Rsq	Expl,Dev	GCV	edf	P	ΔAIC
mw_NDWI2	1,77803	1,34E-01	0,166426	-0,22922	NA	0,03116	0
s(mw_NDWI2)	2,955434	1,66E-01	0,217374	1,798726	1,65525	0,070579	1,177404
null	4,354945	0	0	2,096771	NA	NA	2,576915
mw_altim	4,40535	4,92E-02	0,084422	7,68766	NA	0,133627	2,62732
s(mw_altim)	4,405388	4,92E-02	0,084423	3,090951	1,00001	0,13363	2,627358
mw_rugged	5,467188	1,25E-02	0,049034	5,862726	NA	0,25745	3,689158
s(mw_rugged)	5,467206	1,25E-02	0,049034	3,583947	1,000004	0,257452	3,689176
mw_MSAVI2b	5,532181	1,02E-02	0,046824	1,163253	NA	0,268733	3,754151
northing	5,724775	3,33E-03	0,040245	3,215069	NA	0,306026	3,946745
s(northing)	5,724816	3,33E-03	0,040245	3,703543	1,000008	0,30603	3,946786
mw_slope	5,84762	-1,05E-03	0,036025	5,630938	NA	0,333351	4,06959
s(mw_slope)	5,847645	-1,05E-03	0,036025	3,760577	1,000005	0,333354	4,069615
easting	6,85465	-3,77E-02	0,000725	3,784479	NA	0,891847	5,07662
s(easting)	6,854707	-3,77E-02	0,000725	4,228127	1,000014	0,89189	5,076677
s(mw_MSAVI2b)	7,328012	8,40E-02	0,161698	3,599827	2,289238	0,358132	5,549982

Number of species HL

Variable	AICc	Rsq	Expl,Dev	GCV	edf	P	ΔAIC
easting	79,54602	0,080922	0,114962	37,53405	NA	0,077556	0
s(easting)	79,54622	0,080921	0,114962	37,97771	1,000042	0,077564	0,0002
mw_altim	79,85058	0,07087	0,105283	42,7158	NA	0,092066	0,30456
null	80,44551	0	0	38,78329	NA	NA	0,89949
mw_rugged	80,5488	0,04741	0,082691	40,72205	NA	0,137862	1,00278
s(mw_rugged)	80,54896	0,047409	0,082692	38,44328	1,000033	0,137871	1,00294
mw_slope	80,65211	0,043889	0,0793	40,36159	NA	0,146575	1,10609
s(mw_slope)	80,65234	0,043887	0,079301	38,49125	1,000045	0,146589	1,10632
s(mw_altim)	80,84662	0,09632	0,146925	38,07177	1,511984	0,172607	1,3006
mw_NDWI2	81,24998	0,023254	0,05943	36,66847	NA	0,211253	1,70396
s(mw_NDWI2)	81,2501	0,023253	0,05943	38,76882	1,000024	0,211263	1,70408
northing	81,5501	0,012728	0,049294	38,41969	NA	0,256161	2,00408
s(northing)	81,55041	0,012728	0,049297	38,90817	1,000074	0,256193	2,00439
mw_MSAVI2b	82,8852	-0,03549	0,002864	37,07716	NA	0,786801	3,33918
s(mw_MSAVI2b)	83,97646	-0,01076	0,045072	39,50421	1,491374	0,81885	4,43044

Number of species LL

Variable	AICc	Rsq	Expl,Dev	GCV	edf	P	ΔAIC
mw_NDWI2	127,4562	0,399689	0,421922	58,12137	NA	0,000184	0
s(mw_NDWI2)	127,4563	0,399689	0,421923	60,22172	1,000017	0,000185	0,0001
mw_altim	135,2501	0,207017	0,236387	68,43701	NA	0,008709	7,7939
s(mw_altim)	136,1924	0,239785	0,285915	63,70411	1,638354	0,019335	8,7362
mw_MSAVI2b	136,8587	0,160125	0,191232	62,1363	NA	0,019963	9,4025
s(mw_MSAVI2b)	136,9383	0,160983	0,192869	64,58705	1,026122	0,021685	9,4821
null	140,2815	0	0	67,63281	NA	NA	12,8253
mw_slope	141,5817	0,005808	0,04263	68,65034	NA	0,291817	14,1255
mw_rugged	141,9001	-0,00556	0,031682	69,20658	NA	0,364839	14,4439
s(mw_slope)	142,3654	0,024413	0,073653	66,74484	1,362741	0,419479	14,9092
northing	142,4899	-0,02697	0,011067	66,71318	NA	0,594191	15,0337
easting	142,7945	-0,0382	0,000251	66,89942	NA	0,93628	15,3383
s(mw_rugged)	142,892	0,03626	0,095346	66,7994	1,655338	0,427092	15,4358
s(easting)	143,012	-0,03505	0,00615	67,34209	1,07475	0,973191	15,5558
s(northing)	143,3106	0,266529	0,389227	67,36126	4,516664	0,128147	15,8544

Robustness HL

Variable	AICc	Rsq	Expl,Dev	GCV	edf	P	ΔAIC
s(mw_altim)	-62,3704	0,250385	0,311574	-28,6073	2,203929	0,031168	0
mw_altim	-61,5572	0,122917	0,155402	-22,9378	NA	0,037915	0,81312
northing	-61,092	0,108223	0,141252	-27,807	NA	0,048724	1,27832
s(northing)	-61,0917	0,108224	0,141256	-27,3185	1,000093	0,048736	1,27869
mw_NDWI2	-61,0182	0,105869	0,138985	-29,3846	NA	0,050718	1,35216
s(mw_NDWI2)	-61,0181	0,105869	0,138985	-27,2843	1,000027	0,050722	1,35228
null	-59,3482	0	0	-28,6172	NA	NA	3,02216
mw_rugged	-58,0549	0,006053	0,042866	-23,6297	NA	0,29046	4,31544
s(mw_rugged)	-58,0547	0,006053	0,042868	-25,9084	1,000063	0,290489	4,3157
mw_slope	-57,9829	0,003494	0,040402	-24,0047	NA	0,305067	4,38742
s(mw_slope)	-57,9828	0,003494	0,040402	-25,875	1,00002	0,305077	4,38752
easting	-57,98	0,00339	0,040302	-26,3173	NA	0,30568	4,39035
mw_MSAVI2b	-57,5865	-0,01071	0,02672	-28,1419	NA	0,405898	4,78384
s(easting)	-57,418	0,01403	0,058841	-25,8883	1,227118	0,410434	4,95235
s(mw_MSAVI2b)	-56,0504	0,095115	0,180292	-25,8512	2,541506	0,335352	6,31995

Robustness LL

Variable	AICc	Rsq	Expl,Dev	GCV	edf	P	ΔAIC
mw_altim	-89,6565	0,499338	0,517881	-35,9839	NA	1,59E-05	0
s(mw_altim)	-89,3182	0,561253	0,599798	-41,1319	2,371991	5,90E-05	0,33827
s(mw_NDWI2)	-78,4589	0,403632	0,472946	-36,2444	3,138112	5,69E-03	11,19756
mw_NDWI2	-75,6166	0,17337	0,203986	-36,1624	NA	1,58E-02	14,03993
northing	-72,1938	0,065884	0,100481	-32,9614	NA	1,00E-01	17,46275
s(northing)	-72,1917	0,065908	0,100527	-32,4729	1,000667	1,00E-01	17,46483
null	-71,7487	0	0	-34,5961	NA	NA	17,90782
s(mw_rugged)	-70,7009	0,143173	0,217125	-32,4866	2,330344	1,68E-01	18,9556
s(easting)	-70,069	0,107296	0,179595	-32,0499	2,186681	2,63E-01	19,58749
mw_rugged	-69,9089	-0,01354	0,024003	-29,1333	NA	4,31E-01	19,74756
s(mw_slope)	-69,8679	0,101089	0,173189	-32,0161	2,165617	2,73E-01	19,78858
mw_MSAVI2b	-69,6993	-0,02115	0,016668	-33,7657	NA	5,13E-01	19,95719
s(mw_MSAVI2b)	-69,6991	-0,02115	0,016669	-31,3148	1,000046	5,13E-01	19,9574
mw_slope	-69,6688	-0,02227	0,015594	-29,4302	NA	5,27E-01	19,98774
easting	-69,4526	-0,03019	0,007964	-31,6439	NA	6,52E-01	20,20394

Modularity

Variable	AICc	Rsq	Expl,Dev	GCV	edf	P	ΔAIC
mw_NDWI2	-38,9604	0,103918	0,137106	-19,1435	NA	0,052432	0
s(mw_NDWI2)	-38,9599	0,103923	0,137116	-17,0431	1,000161	0,052454	0,00051
mw_MSAVI2b	-38,2835	0,081991	0,115992	-19,1797	NA	0,076155	0,67688
s(mw_MSAVI2b)	-38,2835	0,081991	0,115992	-16,7289	1,000004	0,076156	0,6769
null	-37,3514	0	0	-18,0117	NA	NA	1,60897
easting	-36,1491	0,009275	0,045969	-16,1815	NA	0,273257	2,81133
s(easting)	-36,1489	0,009275	0,045971	-15,7379	1,000049	0,273279	2,81153
mw_altim	-34,9438	-0,0343	0,004005	-10,5816	NA	0,749016	4,0166
northing	-34,8763	-0,0368	0,001601	-15,6354	NA	0,839806	4,08411
s(northing)	-34,8761	-0,0368	0,001603	-15,1469	1,000042	0,839891	4,08427
mw_slope	-34,8393	-0,03817	0,00028	-13,2594	NA	0,932651	4,12113
mw_rugged	-34,8324	-0,03843	3,52E-05	-12,8478	NA	0,976111	4,12799
s(mw_slope)	-34,1737	0,022616	0,085734	-15,4025	1,743626	0,505758	4,78664
s(mw_altim)	-34,087	-0,0077	0,046347	-15,2498	1,448021	0,69716	4,87341
s(mw_rugged)	-33,9615	0,012262	0,074063	-15,3251	1,689331	0,5658	4,99886

Bird mean abundance

Variable	AICc	Rsq	Expl,Dev	GCV	edf	P	ΔAIC
mw_MSAVI2b	134,5653	0,78550739	7,92E-01	62,04559	NA	9,21235E-12	-0,0003
s(mw_MSAVI2b)	134,5656	0,7855071	7,92E-01	64,29705	1,000049	0	0
mw_NDWI2	158,4105	0,54811023	5,63E-01	73,57265	NA	7,70018E-07	23,8449
s(mw_NDWI2)	159,2381	0,5726548	5,99E-01	75,25514	1,877432	5,18063E-06	24,6725
null	182,4346	0	0,00E+00	88,45381	NA	NA	47,869
mw_rugged	182,6865	0,03506286	6,62E-02	89,18011	NA	1,55E-01	48,1209
northing	183,1962	0,01957204	5,12E-02	86,58064	NA	2,13E-01	48,6306
s(northing)	183,1965	0,01957143	5,12E-02	87,09276	1,000081	2,13E-01	48,6309
mw_slope	183,338	0,01521748	4,70E-02	89,08221	NA	2,33E-01	48,7724
s(mw_rugged)	183,5784	0,08763688	1,43E-01	86,62532	1,884223	2,27E-01	49,0128
s(mw_slope)	184,0259	0,09664197	1,61E-01	86,82897	2,216855	2,76E-01	49,4603
mw_altim	184,5154	-0,02169119	1,13E-02	92,24877	NA	5,63E-01	49,9498
easting	184,839	-0,03207572	1,22E-03	87,41182	NA	8,50E-01	50,2734
s(mw_altim)	184,8973	-0,01595779	2,17E-02	87,70551	1,149104	6,78E-01	50,3317
s(easting)	185,1725	-0,02717286	1,02E-02	87,8589	1,128323	9,19E-01	50,6069

Bird abundance variation

Variable	AICc	Rsq	Expl,Dev	GCV	edf	P	ΔAIC
mw_MSAVI2b	80,10077	0,4340828	0,452338193	36,51533	NA	2,48047E-05	-0,34903
s(mw_MSAVI2b)	80,4498	0,43688803	0,457481975	38,76246	1,133722	5,56781E-05	0
mw_NDWI2	91,14144	0,20091371	0,226690683	42,04026	NA	0,005877164	10,69164
s(mw_NDWI2)	91,14165	0,20091302	0,226691163	43,9421	1,000044	0,005878535	10,69185
easting	93,40624	0,14230908	0,169976532	44,55272	NA	0,01903691	12,95644
s(easting)	93,40638	0,14230895	0,169977351	45,00371	1,000034	0,01903912	12,95658
null	96,92453	0	0	47,03486	NA	NA	16,47473
mw_altim	97,19644	0,03445984	0,065606297	51,31802	NA	1,57E-01	16,74664
s(mw_altim)	97,19664	0,03445894	0,06560674	46,78038	1,000042	1,57E-01	16,74684
northing	99,34125	-0,03247377	0,000831832	47,27365	NA	8,75E-01	18,89145
s(northing)	99,34136	-0,03247443	0,000831938	47,78575	1,000022	8,76E-01	18,89156
mw_rugged	99,34419	-0,03256849	0,000740169	50,11339	NA	8,82E-01	18,89439
s(mw_rugged)	99,34454	-0,03256658	0,000745452	47,78713	1,000103	8,83E-01	18,89474
mw_slope	99,36432	0,03321843	0,000111195	49,71956	NA	9,54E-01	18,91452
s(mw_slope)	101,31093	0,1219926	0,224088202	48,1488	3,604712	3,60E-01	20,86113

Plant mean abundance

Variable	AICc	Rsq	Expl,Dev	GCV	edf	P	ΔAIC
s(mw_NDWI2)	271,5343	0,795888	8,20E-01	128,1171	3,589484	0	-0,4912
mw_NDWI2	272,0255	0,742546	7,51E-01	126,8297	NA	1,46E-10	0
mw_MSAVI2b	297,5001	0,429268	4,48E-01	138,4213	NA	2,83E-05	25,4746
s(mw_MSAVI2b)	297,501	0,429267	4,48E-01	140,6728	1,000229	2,86E-05	25,4755
s(mw_altim)	309,0882	0,279686	3,39E-01	145,5381	2,534112	0,015658	37,0627
s(mw_rugged)	312,4013	0,246805	3,24E-01	146,9834	3,18941	0,047705	40,3758
mw_altim	312,893	0,076705	1,06E-01	152,4258	NA	0,068334	40,8675
s(mw_slope)	312,901	0,233909	3,13E-01	147,277	3,184562	0,057728	40,8755
northing	313,8569	0,048469	7,92E-02	147,8279	NA	0,11876	41,8314
s(northing)	313,8587	0,048477	7,92E-02	148,34	1,000513	0,118889	41,8332
null	314,0527	0	0	152,2063	NA	NA	42,0272
s(easting)	315,1798	0,087221	1,44E-01	148,4283	1,939	2,04E-01	43,1543
easting	315,4288	0,000563	3,28E-02	148,6258	NA	3,21E-01	43,4033
mw_slope	316,4935	-0,03325	8,17E-05	151,4988	NA	9,61E-01	44,468
mw_rugged	316,4959	-0,03333	3,82E-06	151,9033	NA	9,92E-01	44,4704

Plant abundance variation

Variable	AICc	Rsq	Expl,Dev	GCV	edf	P	ΔAIC
mw_NDWI2	219,715	0,351376	3,72E-01	102,3091	NA	0,000209	-0,0004
s(mw_NDWI2)	219,7154	0,351374	3,72E-01	104,211	1,000071	0,000209	0
s(mw_altim)	220,4812	0,41429	4,66E-01	104,2919	2,717878	0,001079	0,7658
mw_altim	228,1171	0,15662	1,84E-01	112,6871	NA	0,014348	8,4017
mw_MSAVI2b	231,321	0,067807	9,79E-02	107,3998	NA	0,081259	11,6056
s(mw_MSAVI2b)	232,0075	0,128954	1,85E-01	109,3513	1,978833	0,12982	12,2921
null	232,1738	0	0	112,5462	NA	NA	12,4584
s(mw_slope)	232,5043	0,133197	1,96E-01	109,5521	2,241613	0,132567	12,7889
s(mw_rugged)	232,5544	0,135128	1,98E-01	109,5278	2,270735	0,1332	12,839
mw_rugged	233,8571	-0,00908	2,35E-02	113,1663	NA	0,402522	14,1417
mw_slope	233,9329	-0,01147	2,12E-02	112,7986	NA	0,427019	14,2175
northing	233,9641	-0,01246	2,02E-02	110,3781	NA	0,437757	14,2487
s(northing)	233,9649	-0,01245	2,02E-02	110,8902	1,000225	0,437895	14,2495
easting	234,617	-0,03333	3,23E-06	110,7453	NA	0,992215	14,9016
s(easting)	235,3605	-0,00976	3,74E-02	111,1211	1,447695	0,734922	15,6451

Table XVII: Multivariated Model selection tables for each metric, showing the AICc values used in the selecting process of the final model for each metric.

Metric	Model Codes	AICc
web asymmetry	gam(web.asymmetry ~ mw_NDWI2, method="REML")	-31.83601
	gam(web.asymmetry ~ mw_NDWI2 + mw_slope, method="REML")	-30.6692
	gam(web.asymmetry ~ mw_slope + s(mw_altim), family='gaussian', method="REML")	-29.5732
	gam(web.asymmetry ~ mw_slope, family='gaussian', method="REML")	-29.4028
	gam(web.asymmetry ~ mw_NDWI2 + s(mw_altim), family='gaussian', method="REML")	-29.1008
	gam(web.asymmetry ~ mw_NDWI2 + mw_slope + s(mw_altim), family='gaussian', method="REML")	-27.7731
	gam(web.asymmetry ~ s(mw_altim), family='gaussian', method="REML")	-26.9410
	gam(web.asymmetry ~ 1, family='gaussian', method="REML")	-25.7365
Weighted NODF	gam(weighted.NODF ~ s(mw_NDWI2) , family='gaussian', method="REML")	239.9208
	gam(weighted.NODF ~ s(mw_NDWI2) + mw_altim, family='gaussian', method="REML")	242.9095
	gam(weighted.NODF ~ mw_altim, family='gaussian', method="REML")	245.0934
	gam(weighted.NODF ~ 1, family='gaussian', method="REML")	246.2614
interaction strength asymmetry	gam(interaction.strength.asymmetry ~ mw_MSAVI2b , family='gaussian', method="REML")	-15.1224
	gam(interaction.strength.asymmetry ~ mw_rugged , family='gaussian', method="REML")	-15.0748
	gam(interaction.strength.asymmetry ~ mw_MSAVI2b + s(mw_altim) , family='gaussian', method="REML")	-14.4654
	gam(interaction.strength.asymmetry ~ mw_MSAVI2b + mw_rugged , family='gaussian', method="REML")	-13.5028
	gam(interaction.strength.asymmetry ~ mw_MSAVI2b + mw_rugged + s(mw_altim) , family='gaussian', method="REML")	-13.5028
	gam(interaction.strength.asymmetry ~ mw_rugged + s(mw_altim) , family='gaussian', method="REML")	-12.0358
	gam(interaction.strength.asymmetry ~ s(mw_altim) , family='gaussian', method="REML")	-10.6908
	gam(interaction.strength.asymmetry ~ 1 , family='gaussian', method="REML")	-10.4793
specialisation asymmetry	gam(specialisation.asymmetry ~ s(mw_altim) + mw_rugged , family='gaussian', method="REML")	-21.2041
	gam(specialisation.asymmetry ~ s(mw_altim) , family='gaussian', method="REML")	-19.7612
	gam(specialisation.asymmetry ~ s(mw_altim) + mw_MSAVI2b , family='gaussian', method="REML")	-19.6144
	gam(specialisation.asymmetry ~ s(mw_altim) + mw_rugged + mw_MSAVI2b , family='gaussian', method="REML")	-17.5093
	gam(specialisation.asymmetry ~ s(mw_altim) + mw_rugged + northing, family='gaussian', method="REML")	-17.4430

	gam(specialisation.asymmetry ~ s(mw_altim) + northing, family='gaussian', method="REML")	-17.4359
	gam(specialisation.asymmetry ~ mw_rugged , family='gaussian', method="REML")	-16.4585
	gam(specialisation.asymmetry ~ s(mw_altim) + mw_MSAVI2b + northing, family='gaussian', method="REML")	-16.0960
	gam(specialisation.asymmetry ~ mw_rugged + northing, family='gaussian', method="REML")	-14.6313
	gam(specialisation.asymmetry ~ mw_rugged + mw_MSAVI2b, family='gaussian', method="REML")	-13.9245
	gam(specialisation.asymmetry ~ s(mw_altim) + mw_rugged + mw_MSAVI2b + northing, family='gaussian', method="REML")	-13.3537
	gam(specialisation.asymmetry ~ mw_rugged + mw_MSAVI2b + northing, family='gaussian', method="REML")	-11.8731
	gam(specialisation.asymmetry ~ mw_MSAVI2b , family='gaussian', method="REML")	-11.0022
	gam(specialisation.asymmetry ~ northing, family='gaussian', method="REML")	-10.4857
	gam(specialisation.asymmetry ~ mw_MSAVI2b + northing, family='gaussian', method="REML")	-10.1729
	gam(specialisation.asymmetry ~ 1, family='gaussian', method="REML")	-9.77871
Linkage density	glm(linkage.density ~ mw_NDWI2 , family='gaussian')	40.56193
	glm(linkage.density ~ mw_NDWI2 + mw_altim, family='gaussian')	41.155
	glm(linkage.density ~ mw_altim, family='gaussian')	59.03528
	glm(linkage.density ~ 1, family='gaussian')	62.60994
	gam(linkage.density ~ s(mw_NDWI2) , family='gaussian', method="REML")	41.3712
	gam(linkage.density ~ s(mw_NDWI2) + mw_altim, family='gaussian', method="REML")	42.11527
	gam(linkage.density ~ mw_altim, family='gaussian', method="REML")	59.03528
	gam(linkage.density ~ 1 , family='gaussian', method="REML")	62.60994
Shannon diversity	glm(Shannon.diversity ~ mw_NDWI2 , family='gaussian')	22.7797
	glm(Shannon.diversity ~ mw_NDWI2 + mw_altim, family='gaussian')	22.50388
	glm(Shannon.diversity ~ mw_NDWI2 , family='gaussian')	22.7797
	glm(Shannon.diversity ~ 1 , family='gaussian')	30.45394
H2	glm(H2 ~ mw_NDWI2 , family='gaussian')	1.77803
	glm(H2 ~ 1 , family='gaussian')	4.354945
	gam(H2 ~ s(mw_NDWI2) , family='gaussian', method="REML")	2.955434
	gam(H2 ~ 1 , family='gaussian', method="REML")	4.354945
Number of species HL	glm(number.of.species.HL ~ 1, family='poisson')	100.5145
	glm(number.of.species.HL ~ easting , family='poisson')	102.1511

	glm(number.of.species.HL ~ mw_altim, family='poisson')	102.2194
	glm(number.of.species.HL ~ easting + mw_altim, family='poisson')	103.9247
Number of species LL	glm(number.of.species.LL ~ mw_NDWI2 , family='poisson')	127.889
	glm(number.of.species.LL ~ mw_NDWI2 + mw_altim, family='poisson')	128.7442
	glm(number.of.species.LL ~ mw_altim, family='poisson')	132.9247
	glm(number.of.species.LL ~ 1, family='poisson')	137.0065
Robustness HL	gam(robustness.HL ~ s(mw_altim) + mw_NDWI2, family='gaussian', method="REML")	-65.1275
	gam(robustness.HL ~ s(mw_altim) + northing + mw_NDWI2, family='gaussian', method="REML")	-64.3261
	gam(robustness.HL ~ northing + mw_NDWI2, family='gaussian', method="REML")	-63.4803
	gam(robustness.HL ~ s(mw_altim), family='gaussian', method="REML")	-62.3703
	gam(robustness.HL ~ s(mw_altim) + northing , family='gaussian', method="REML")	-61.2039
	gam(robustness.HL ~ northing, family='gaussian', method="REML")	-61.0920
	gam(robustness.HL ~ mw_NDWI2, family='gaussian', method="REML")	-61.0181
	gam(robustness.HL ~ 1, family='gaussian', method="REML")	-59.3481
Robustness LL	gam(robustness.LL ~ mw_altim , family='gaussian', method="REML")	-89.6565
	gam(robustness.LL ~ mw_altim + s(mw_NDWI2) , family='gaussian', method="REML")	-88.3789
	gam(robustness.LL ~ mw_altim + northing, family='gaussian', method="REML")	-87.7694
	gam(robustness.LL ~ mw_altim + s(mw_NDWI2) + northing, family='gaussian', method="REML")	-86.4249
	gam(robustness.LL ~ s(mw_NDWI2), family='gaussian', method="REML")	-78.4589
	gam(robustness.LL ~ s(mw_NDWI2) + northing, family='gaussian', method="REML")	-77.0478
	gam(robustness.LL ~ northing, family='gaussian', method="REML")	-72.1937
	gam(robustness.LL ~ 1, family='gaussian', method="REML")	-71.7486
	gam(robustness.LL ~ s(mw_altim) + s(mw_NDWI2) , family='gaussian', method="REML")	-89.7117
	gam(robustness.LL ~ s(mw_altim) , family='gaussian', method="REML")	-89.3182
	gam(robustness.LL ~ s(mw_altim) + s(mw_NDWI2) + northing , family='gaussian', method="REML")	-86.7484
	gam(robustness.LL ~ s(mw_altim) + northing , family='gaussian', method="REML")	-86.7228
	gam(robustness.LL ~ s(mw_NDWI2) , family='gaussian', method="REML")	-78.4589
	gam(robustness.LL ~ s(mw_NDWI2) + northing , family='gaussian', method="REML")	-77.0478
	gam(robustness.LL ~ northing , family='gaussian', method="REML")	-72.1937

	gam(robustness.LL ~ 1 , family='gaussian', method="REML")	-71.7486
Modularity	glm(modularity ~ mw_NDWI2 , family='gaussian')	-38.9603
	glm(modularity ~ 1 , family='gaussian')	-37.3514
Bird mean abundance	glm(m_aves ~ mw_MSAVI2b, data=media_aves, family='gaussian', na.action="na.omit")	134.5653
	glm(m_aves ~ 1, data=media_aves, family='gaussian', na.action="na.omit")	182.4346
Bird abundance variation	glm(sd_aves ~ mw_MSAVI2b, data=sdev_aves, family='gaussian', na.action="na.omit")	80.10077
	glm(sd_aves ~ easting, data=sdev_aves, family='gaussian', na.action="na.omit")	93.40624
	glm(sd_aves ~ mw_MSAVI2b + easting, data=sdev_aves, family='gaussian', na.action="na.omit")	71.01846
	glm(sd_aves ~ 1, data=sdev_aves, family='gaussian', na.action="na.omit")	96.92453
Plant mean abundance	gam(m_plant ~ s(mw_altim), data=media_plantas, family='gaussian', method="REML", na.action="na.omit")	309.0882
	gam(m_plant ~ s(mw_rugged), data=media_plantas, family='gaussian', method="REML", na.action="na.omit")	312.8569
	gam(m_plant ~ s(mw_NDWI2), data=media_plantas, family='gaussian', method="REML", na.action="na.omit")	271.5343
	gam(m_plant ~ northing , data=media_plantas, family='gaussian', method="REML", na.action="na.omit")	313.8569
	gam(m_plant ~ s(mw_altim) + s(mw_rugged), data=media_plantas, family='gaussian', method="REML", na.action="na.omit")	310.8168
	gam(m_plant ~ s(mw_altim) + s(mw_NDWI2), data=media_plantas, family='gaussian', method="REML", na.action="na.omit")	272.2845
	gam(m_plant ~ s(mw_altim) + northing , data=media_plantas, family='gaussian', method="REML", na.action="na.omit")	308.8411
	gam(m_plant ~ s(mw_rugged) + s(mw_NDWI2), data=media_plantas, family='gaussian', method="REML", na.action="na.omit")	276.5806
	gam(m_plant ~ s(mw_rugged) + northing , data=media_plantas, family='gaussian', method="REML", na.action="na.omit")	313.2016
	gam(m_plant ~ s(mw_NDWI2) + northing , data=media_plantas, family='gaussian', method="REML", na.action="na.omit")	269.3400
	gam(m_plant ~ s(mw_altim) + s(mw_rugged) + s(mw_NDWI2), data=media_plantas, family='gaussian', method="REML", na.action="na.omit")	287.9604
	gam(m_plant ~ s(mw_altim) + s(mw_rugged) + northing , data=media_plantas, family='gaussian', method="REML", na.action="na.omit")	312.1593
	gam(m_plant ~ s(mw_altim) + s(mw_NDWI2) + northing , data=media_plantas, family='gaussian', method="REML", na.action="na.omit")	272.2596
	gam(m_plant ~ s(mw_rugged) + s(mw_NDWI2) + northing , data=media_plantas, family='gaussian', method="REML", na.action="na.omit")	273.5368

Plant abundance variation	gam(m_plant ~ s(mw_altim) + s(mw_rugged) + s(mw_NDWI2) + northing , data=media_plantas, family='gaussian', method="REML", na.action="na.omit")	280.9388
	gam(m_plant ~ 1 , data=media_plantas, family='gaussian', method="REML", na.action="na.omit")	314.0527
	gam(sd_plant ~ mw_NDWI2, data=sdev_plant, family='gaussian', method="REML", na.action="na.omit")	219.7150
	gam(sd_plant ~ s(mw_altim), data=sdev_plant, family='gaussian', method="REML", na.action="na.omit")	220.4812
	gam(sd_plant ~ mw_NDWI2 + s(mw_altim), data=sdev_plant, family='gaussian', method="REML", na.action="na.omit")	215.9076
	gam(sd_plant ~ 1, data=sdev_plant, family='gaussian', method="REML", na.action="na.omit")	232.1738